Microtubule-dependent endosomal sorting of clathrin-independent cargo by Hook1

Lymarie Maldonado-Báez,[1] Nelson B. Cole,[1] Helmut Krämer,[2,3] and Julie G. Donaldson[1]

[1]Laboratory of Cell Biology, Cell Biology and Physiology Center, National Heart, Lung and Blood Institute, National Institutes of Health, Bethesda, MD 20892
[2]Department of Cell Biology and [3]Department of Neuroscience, University of Texas Southwestern Medical Center, Dallas, TX 75390

Many plasma membrane (PM) proteins enter cells nonselectively through clathrin-independent endocytosis (CIE). Here, we present evidence that cytoplasmic sequences in three CIE cargo proteins—CD44, CD98, and CD147—were responsible for the rapid sorting of these proteins into endosomal tubules away from endosomes associated with early endosomal antigen 1 (EEA1). We found that Hook1, a microtubule- and cargo-tethering protein, recognized the cytoplasmic tail of CD147 to help sort it and CD98 into Rab22a-dependent tubules associated with recycling. Depletion of Hook1 from cells altered trafficking of CD44, CD98, and CD147 toward EEA1 compartments and impaired the recycling of CD98 back to the PM. In contrast, another CIE cargo protein, major histocompatibility complex class I, which normally traffics to EEA1 compartments, was not affected by depletion of Hook1. Loss of Hook1 also led to an inhibition of cell spreading, implicating a role for Hook1 sorting of specific CIE cargo proteins away from bulk membrane and back to the PM.

Introduction

Endocytosis is a fundamental cellular process involved in nutrient uptake, receptor signaling, and turnover of plasma membrane (PM) proteins and lipids. After endocytosis, membrane and content is subsequently sorted and trafficked to the appropriate destination: to lysosomes for degradation or the PM and other organelles for reuse. Although clathrin-mediated endocytosis (CME) has been widely studied, with details of mechanisms for cargo selection, internalization, and vesicle formation well established (Conner and Schmid, 2003; Traub, 2009), much less is known about mechanisms for endocytosis without clathrin (Mayor and Pagano, 2007; Howes et al., 2010b; Sandvig et al., 2011). There is evidence of distinct endocytosis requirements for certain cargoes in particular cell types, leading to an apparent variety of entry mechanisms including the Arf6-associated mode of clathrin-independent endocytosis (CIE; Donaldson et al., 2009) and the CLIC/GEEC pathway (Mayor and Pagano, 2007). A common feature of both of these forms of CIE is their independence of clathrin and dynamin, and dependence on membrane cholesterol. CIE also occurs in worms (Balklava et al., 2007) and yeast (Prosser et al., 2011), which indicates that it is a conserved cellular activity.

The list of proteins entering cells by CIE is growing rapidly. It includes: major histocompatibility complex class I (MHCI) proteins (Radhakrishna and Donaldson, 1997); peptide-loaded class II (Walseng et al., 2008); CD1a (Barral et al., 2008); E-cadherin (Paterson et al., 2003); β1-integrin (Powelka et al., 2004); syndecan 1 (Zimmermann et al., 2005); the potassium channel Kir3.4 (Gong et al., 2007); the TRP-like calcium channel mucolipin 2 (Karacsonyi et al., 2007); glycosyl phosphatidylinositol-anchored proteins (GPI-APs) CD59 and CD55 (Naslavsky et al., 2004; Eyster et al., 2009); and Glut1, ICAM1, CD44, CD98, and CD147 (Eyster et al., 2009). Although most of these cargo proteins have been identified associated with Arf6 endosomes, a recent analysis of the CLIC/GEEC endosome also identified similar sets of cargo proteins (including CD44, CD98, and β1-integrin; Howes et al., 2010a), which suggests that these endosomal systems are closely related.

The entry and intracellular itinerary followed by CIE cargo proteins have been well documented in HeLa cells where MHCI and CD59 are typical endogenous CIE cargo proteins. MHCI and CD59 enter cells in vesicles lacking the transferrin

Correspondence to Julie G. Donaldson: donaldsonj@helix.nih.gov

Abbreviations used in this paper: CIE, clathrin-independent endocytosis; CME, clathrin-mediated endocytosis; EEA1, early endosomal antigen 1; MHCI, major histocompatibility complex class I; PM, plasma membrane; SIM, structured illumination microscopy; TfR, transferrin receptor; TM, transmembrane; Y2H, yeast two-hybrid.

The Rockefeller University Press $30.00
J. Cell Biol. Vol. 201 No. 2 233–247
www.jcb.org/cgi/doi/10.1083/jcb.201208172

receptor (TfR), a typical CME cargo protein, and then several minutes later are observed in classical sorting endosomes containing TfR and the early endosomal antigen 1 (EEA1). From here, MHCI and CD59 are routed either to late endosomes for degradation or back to the cell surface via distinctive tubular endosomes (Radhakrishna and Donaldson, 1997; Naslavsky et al., 2003, 2004). A new group of CIE cargo proteins that includes CD44, CD98, and CD147 follows a different itinerary after endocytosis (Eyster et al., 2009). CD44, CD98, and CD147 enter cells by CIE and then rapidly join recycling tubules; unlike MHCI and CD59, they are not observed in endosomes containing TfR and EEA1 (Eyster et al., 2009). This avoidance of EEA1-associated endosomes leads to prolonged surface lifetimes of CD44, CD98, and CD147 in HeLa cells (Eyster et al., 2011), as these proteins do not readily traffic to late endosomes and lysosomes (Eyster et al., 2009).

The recycling of CIE cargo proteins back to the PM is regulated by numerous factors including several Rab proteins, epsin-homology domain proteins (EHDs; Naslavsky and Caplan, 2011), Arf6, and actin (Grant and Donaldson, 2009). Among the Rab proteins required for recycling, Rab22a localizes to the recycling tubules, and cellular depletion of Rab22a leads to loss of recycling tubules and delayed recycling of CIE cargo (Weigert et al., 2004). The directed Arf6-dependent recycling of this membrane back to the cell surface is important for cell spreading and migration, wound healing, and cancer cell metastasis (Song et al., 1998; Hashimoto et al., 2004; Powelka et al., 2004; Balasubramanian et al., 2007).

The alternative itinerary taken by CD44, CD98, and CD147 that allows them to avoid residence in EEA1 compartments raises the possibility that these proteins might contain signals that allow for their sorting on endosomes. In this study, we examine whether there is information contained within CIE cargo proteins that specifies their intracellular itinerary. We identify endosomal sorting determinants in the cytoplasmic tail of CD147 and show that Hook1 is part of the cellular machinery involved in the direct sorting of these cargo proteins toward recycling.

Results

CD44 and CD147 contain sorting signals that direct them to tubular recycling endosomes and limit their residence in EEA1-associated endosomes

To identify potential sorting determinants in the sequences of CD44 and CD147, we created chimeric proteins, combining sequences from Tac, the α subunit of the interleukin 2 receptor, with those of CD44 and CD147, all type-I membrane proteins. Tac has been used in many studies as a reporter molecule for identifying sorting determinants, enters cells by CIE, and has the same trafficking itinerary as MHCI (Radhakrishna and Donaldson, 1997; Naslavsky et al., 2003). We first compared the itinerary of endogenous CD44 and CD147 and compared it to that of transfected Tac in HeLa cells. Cells were incubated with mouse monoclonal antibodies to CD44, CD147, or Tac at 37°C for 1 h to allow internalization of the antibody-bound protein, and internalized antibody was then detected as described in Materials and methods. CD44 and CD147 were found prominently in internal tubular structures that were largely devoid of EEA1 (Fig. 1 A), as observed previously (Eyster et al., 2009). In contrast, endocytosed Tac was found in discrete punctate structures, some of which colocalized with EEA1 in the juxtanuclear region (Fig. 1 A; Naslavsky et al., 2003). Tac could also be seen in tubular endosomes, but was less prominent than CD44 and CD147.

Next, we created chimeric cargo proteins consisting of the extracellular domain of CD44 or CD147 with the transmembrane (TM) and cytoplasmic, carboxyl-terminal regions of Tac and vice versa (Fig. 1 B). In contrast to the trafficking of endogenous CD44 and CD147, the chimeras harboring the TM and carboxyl-terminal regions of Tac localized to the EEA1-endosomal compartment and were less apparent in the tubular recycling endosomes (Fig. 1 C, CD44-Tac-Tac, CD147-Tac-Tac). However, those chimeras containing the TM and carboxyl-terminal sequences of either CD44 or CD147 were not observed in EEA1-positive endosomes but instead in recycling tubules (Fig. 1 C, Tac-44-44, Tac-147-147). For CD147, we dissected this further and found that the Tac-Tac-147 chimera had a trafficking itinerary similar to CD147. This chimera accumulated in the tubular recycling endosomes and rarely colocalized with EEA1 after 1 h of internalization (Fig. 1 C, Tac-Tac-147), whereas the chimeras containing only the TM domain of CD147 behaved more like Tac (not depicted). Thus, cytoplasmic sequences contained within these CIE cargo proteins are sufficient to rapidly direct these proteins to the tubular recycling endosomes avoiding residence in EEA1-associated endosomes. Although the carboxyl-terminal region of CD147 alone was sufficient to direct Tac trafficking, Tac-Tac-147 was poorly expressed at the PM and thus subsequent mutagenesis was performed on Tac-147-147, hereafter referred to as Tac-CD147.

Conserved amino acids contribute to the sorting of CD147 into the tubular endosome

We noticed two highly conserved clusters of acidic amino acids in the cytoplasmic tail of CD147 (aa 236–246; Fig. 2 A). To investigate the role of these conserved amino acids in the distinct endosomal sorting of CD147, we studied the trafficking of different carboxyl-terminal truncations of the Tac-CD147 chimera. We observed that the Tac-CD147(235) chimera, which lacks the acidic cluster region, colocalized with EEA1 in endosomal structures and only weakly colocalized to the recycling tubules, similar to Tac (Fig. 2, B and C). Conversely, the Tac-CD147 truncations that include the acidic clusters (Tac-CD147(246) and Tac-CD147(261)) exhibited a trafficking itinerary analogous to Tac-CD147 and CD147. These chimeras avoided going to the EEA1-positive endosomes and were directly delivered to the tubular endosomes (Fig. 2, B and C). Mutation of the acidic residues within the cluster to Ala in full-length Tac-CD147 also led to a successive shift from avoiding to localizing to EEA1 compartments (Fig. S1). However, as the chimera with the mutated residues still was observed in recycling tubules, the acidic residues are not the only signal recognized by the sorting machinery.

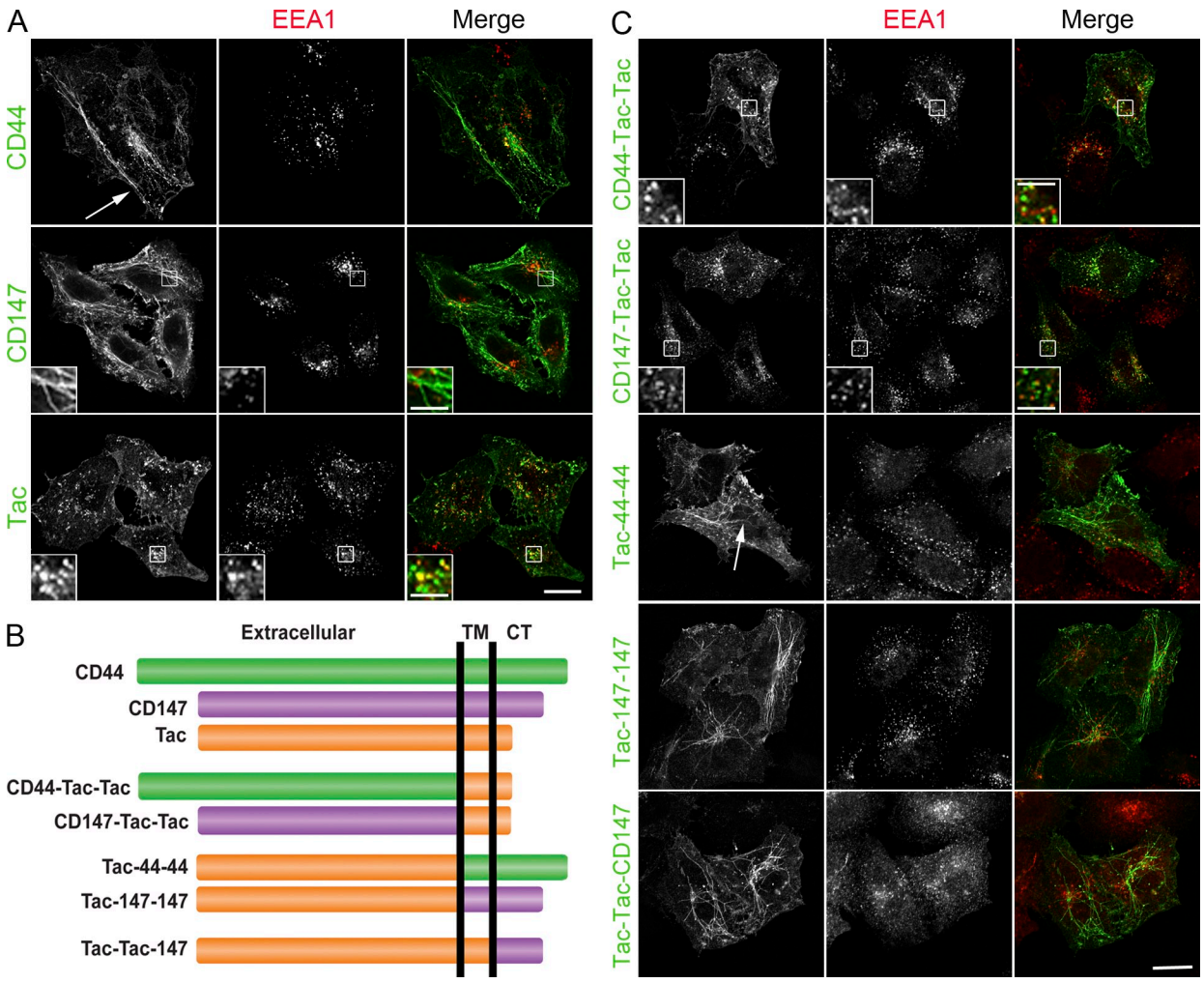

Figure 1. **CD44 and CD147 contain sorting sequences that direct their traffic to recycling tubular endosomes.** (A) HeLa cells were incubated with primary antibodies against endogenous CD44, endogenous CD147, or Tac for 1 h at 37°C to allow internalization of the cargo proteins. After fixation, cells were immunolabeled with antibodies to EEA1, followed by secondary antibodies to detect EEA1 (red) and cargo proteins (green). Insets show enlarged views of the boxed regions. (B) Schematic representation of Tac, CD44, and CD147 chimeras used to identify potential sorting sequences in these CIE cargo proteins. Tac sequences are in orange, CD44 sequences in green, and CD147 sequences in purple. (C) HeLa cells transfected with either Tac or the different chimeric proteins were incubated with anti-CD44, anti–rat CD147, or anti-Tac antibodies for 1 h at 37°C to allow internalization of the antibody-bound cargo. Immunofluorescence analysis of all experiments was performed as described in Materials and methods. Arrows in A and C point to tubular endosomes. Bars: (A and C) 10 µm; (insets) 3 µm.

Recent work from our group demonstrated that CD147 has the ability to avoid degradation in lysosomes by direct delivery to the tubular recycling endosomes (Eyster et al., 2011). Because EEA1-positive endosomes have been considered as preselection compartments for delivery to multivesicular bodies and further degradation of the cargo (Leonard et al., 2008), we sought to investigate whether the cytoplasmic domain of CD147 was sufficient for Tac to evade transport to late endosomes. To test this, we allowed cells to internalize antibody-bound cargo for 1 h, then removed the unbound antibody and chased the cargo in complete media in the presence of ammonium chloride to inhibit lysosomal proteases and block degradation. As expected, Tac accumulated in Lamp1-positive endosomes after 22 h with little antibody-bound Tac remaining at the cell surface (Fig. 2 D, top). In contrast, in addition to some present in lysosomes, a substantial amount of Tac-CD147 and Tac-CD147(261) still remained on the cell surface and in recycling tubules (Fig. 2 D, second and fourth row). However, the truncated mutant, Tac-CD147(235), was efficiently delivered to the Lamp1-positive lysosomes (Fig. 2 D, third row) and was mostly absent from the surface, similar to Tac. These data indicate that the cytoplasmic domain of CD147 is sufficient to redirect the trafficking of Tac to the recycling route, preventing transport to late endosomes. We have also observed that the cytoplasmic portion of CD98, a type-II membrane protein that follows the same trafficking itinerary as CD147 and CD44 (Eyster et al., 2009), also dictates its intracellular itinerary (unpublished data).

Hook1 interacts with the cytoplasmic region of CD147 and colocalizes with CIE cargo proteins in the tubular recycling compartment

To identify proteins interacting with the cytoplasmic domain of CD147, we performed a yeast two-hybrid (Y2H) screen. We used the cytoplasmic tail of CD147 as the bait and a

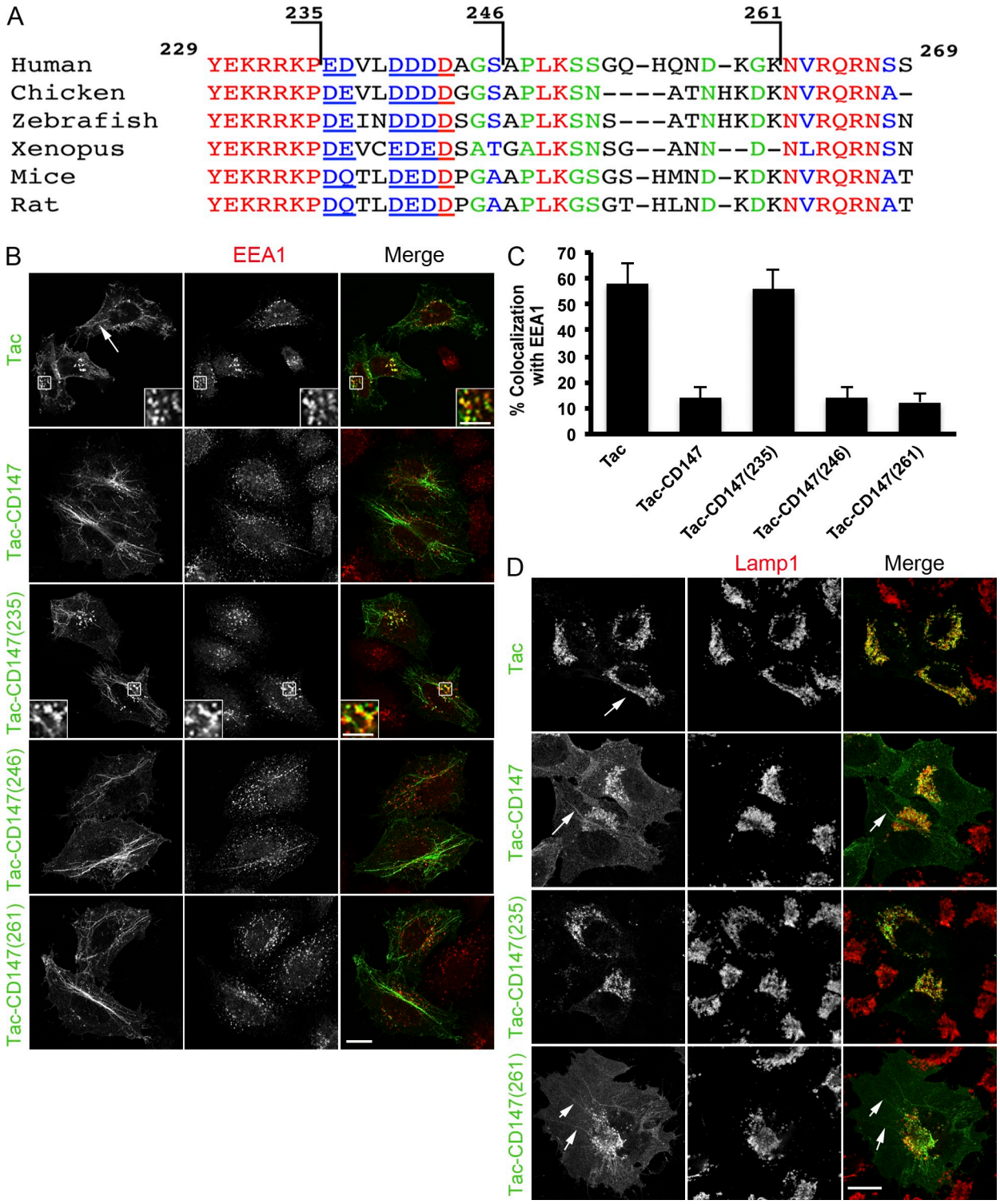

Figure 2. **CD147 cytoplasmic sequence is sufficient for sorting directly into the recycling route.** (A) Sequence alignment of the cytoplasmic tail (carboxyl terminal) of CD147, showing location of the truncated constructs at positions 235, 246, and 261. Identical sequences are highlighted in red, strongly similar in blue, and weakly similar in green. (B) Tac-CD147 carboxyl-terminal truncations were expressed in HeLa cells, and their locations were assessed after internalization for 1 h at 37°C using an anti-Tac antibody. Cells were fixed and processed for immunofluorescence as described in Materials and methods. Insets show enlarged views of the boxed regions. (C) The percentage of colocalization of internal Tac-CD147 truncated chimeras with EEA1 was quantified using MetaMorph software (see Materials and methods). The data presented is the mean of three independent experiments ± SD (error bars). (D) Cells expressing the different Tac-CD147 chimeras were incubated with anti-Tac for 1 h at 37°C. Then the cells were washed with media and chased in media containing 15 mM NH_4Cl for 22 h. The arrow in the top row points to the cell surface. Other arrows point to tubular endosomes. The chimeric proteins were visualized with Alexa Fluor 488–conjugated goat anti–mouse, and late endosomes were visualized with antibodies to Lamp1. Bars: (B and D) 10 µm; (B, insets) 5 µm.

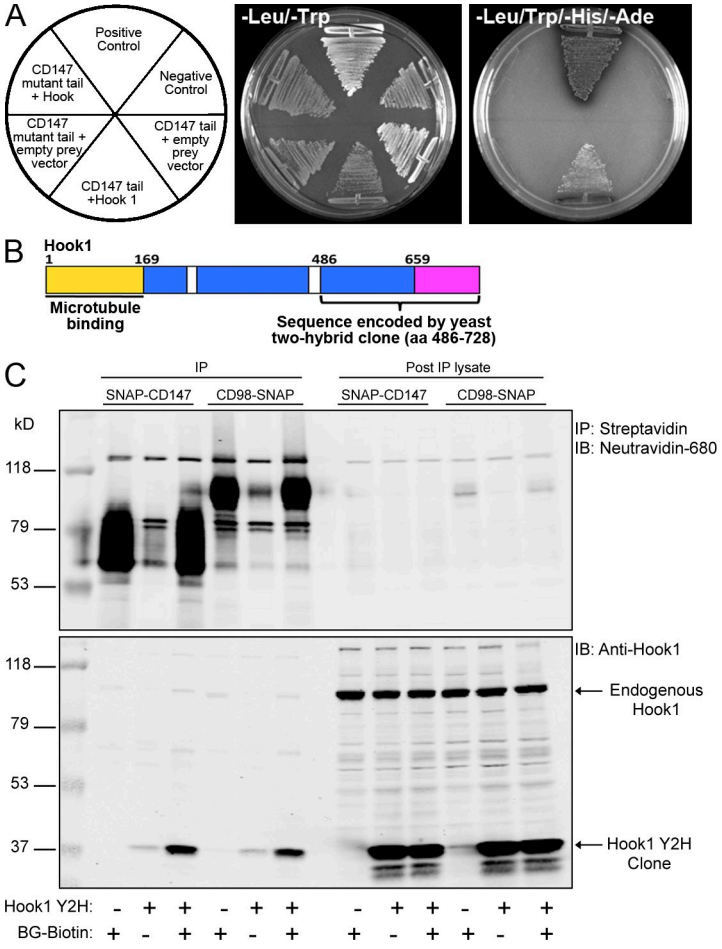

Figure 3. **Hook1 interacts with the cytoplasmic tail of CD147 and CD98 through its carboxyl-terminal region.** (A) Y2H analysis of the interaction between the cytoplasmic sequence of CD147 and the carboxyl-terminal sequence of Hook1. Yeast cells coexpressing CD147 carboxyl-terminal tail or the CD147 carboxyl-terminal acidic-cluster mutant (prey) and the carboxyl-terminal sequence of Hook1 or the pGBKT7 empty vector (bait) were grown on high-stringency plates. Growth on the –Leu/–TRP plate confirmed the expression of bait and prey plasmids (see Materials and methods for details about the Y2H screen). (B) Schematic representation of the domain organization of Hook1 (the amino terminus is shown in yellow; aa 1–168, coiled-coil region in blue; carboxyl terminus in pink, aa 659–728). Y2H clone encoding for amino acids 486–728 of Hook1. (C) BG-biotin–labeled SNAP-CD147 and CD98-SNAP were immunoprecipitated from lysates of cells coexpressing the Hook1 Y2H clone and separated on SDS–PAGE and immunoblotted as described in Materials and methods. The Hook1 Y2H clone was detected with rabbit anti-Hook1 and visualized with goat anti–rabbit 800 (bottom). The biotin-labeled SNAP-CD147 and CD98-SNAP were detected with NeutrAvidin DyLight-680 (top). For post-immunoprecipitation lysate (lanes 7–12), 1/10 of total protein was loaded.

normalized universal human cDNA library as prey. We identified a 694-nucleotide-long cDNA coding for the carboxyl-terminal domain and a portion of the coil-coiled region of the Hook1 protein, hereafter referred to as Hook1-Y2H (Fig. 3, A and B). We isolated the same Hook1 clone nine times in the screen. Directed two-hybrid experiments using a CD147 cytoplasmic tail acidic cluster mutant bait where the acidic residues were mutated to Ala showed no interaction with Hook1-Y2H under high stringency conditions for growth (Fig. 3 A). However, some interaction was observed under low stringency conditions (unpublished data). We did not observe any interaction of Hook1-Y2H with the cytoplasmic tail of CD44 (unpublished data). To confirm the interaction between CD147 and Hook1 in mammalian cells, we tested whether both proteins could be coprecipitated from whole cell lysates. HeLa cells were cotransfected with Hook1-Y2H and SNAP-tagged CD147. We labeled cells expressing SNAP-CD147 with BG-PEG_4-biotin and looked for Hook1 in streptavidin precipitations. The Hook1-Y2H carboxyl-terminal domain associated with SNAP-CD147 (Fig. 3 C). We could also detect an interaction between the Hook1-Y2H domain and CD98-SNAP (Fig. 3 C); however, we did not capture this complex with SNAP-CD44 (not depicted). Unfortunately, we could not detect full-length Hook1, whether endogenous or overexpressed, binding to SNAP-CD147, CD98-SNAP, or endogenous CD147 or CD98.

Hook1 belongs to the Hook protein family (Krämer and Phistry, 1996; Krämer and Phistry, 1999), a group of cytosolic coiled-coil proteins that contain a conserved amino-terminal domain, which can associate with microtubules, a central coiled-coil region important for oligomerization, and a more divergent carboxyl-terminal domain (Fig. 3 B). The carboxyl-terminal domain is thought to mediate the binding of Hook proteins to intracellular organelles. Hook1 is known to localize to cytoplasmic structures devoid of EEA1, Lamp-1, or other organellar markers (Walenta et al., 2001). Hook proteins have been described as factors that facilitate the attachment of organelles to microtubules (Walenta et al., 2001).

We examined the distribution of endogenous Hook1 in HeLa cells using a rabbit anti-Hook1 antibody (Walenta et al., 2001). Endogenous Hook1 partially colocalized with internalized CD147, CD44, and also with CD98. We observed Hook1 with the cargo in the tubular recycling endosomes and on endosomal structures near the tubules (Fig. 4 A). Hook1 showed a distinctive distribution on the tubes, labeling some but not all of the cargo containing tubules (Fig. 4, A and B, and insets). Overexpression of Hook1 did not affect its colocalization with CIE cargo proteins (Fig. 4 B) nor induce any noticeable phenotype. We observed colocalization of HA-Hook1 and the CIE cargo on endosomes, on tubules, and at branching points and swollen regions of the tubular recycling network (Fig. 4 B, bottom).

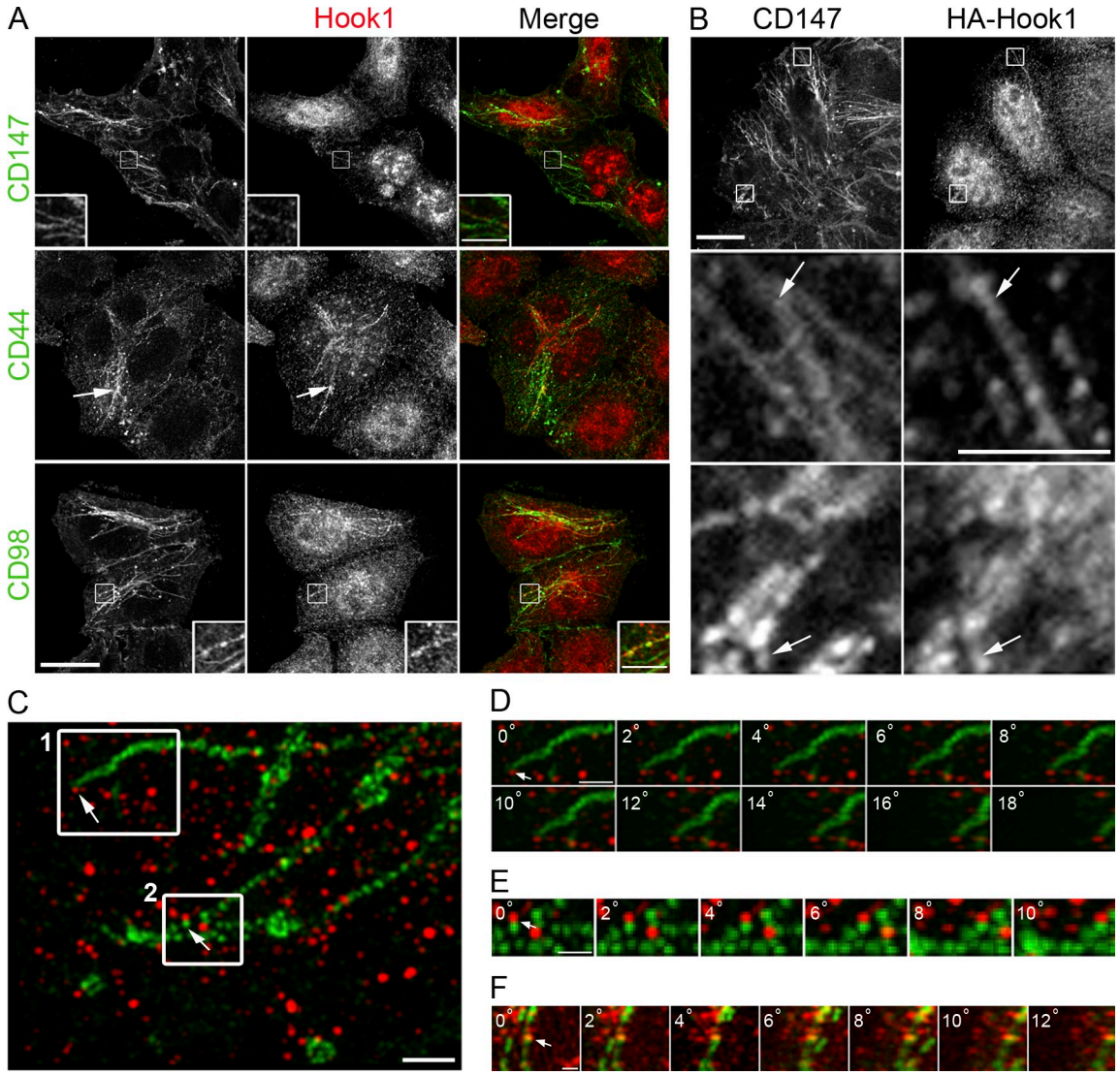

Figure 4. **Hook1 colocalizes with CD44, CD98, and CD147 on tubular endosomes.** (A) HeLa cells were incubated with anti-CD147, anti-CD44, or anti-CD98 for 30 min at 37°C to allow the internalization of the cargo-bound antibodies. After internalization, cells were treated for 1 min with 10 µg/ml digitonin and then fixed. Endogenous Hook1 was localized using a rabbit anti-Hook1 antibody. Arrows point to tubular endosomes. (B) HeLa cells overexpressing HA-Hook1 were incubated with anti-CD147 antibody for 30 min at 37°C and processed for immunofluorescence. Enlargements of the two boxed regions are shown below. Arrows in the middle row indicate tubes, and arrows in the bottom row indicate swollen regions of the tubes. (C) After antibody internalization, endogenous CD147 (green; Alexa Fluor 488) and endogenous Hook1 (red; Alexa Fluor 568) were visualized using super-resolution fluorescence microscopy (SIM). This image is one projection of a 3D SIM image of a region of interest in the cell where CD147 colocalizes with Hook1 on tubular endosomal structures. Insets show enlarged views of the boxed regions. (D) Projection of a 3D image (from C, box 1) from 0° to 18° with 2° increments showing colocalization between CD147 (green) and Hook1 (red) at the end of a tubular endosome. (E) Montage of a 3D image (from C, box 2) from 0° to 10° with 2° increments showing CD147 (green) and Hook1 (red) together on an endosome (F). Endogenous Hook1 (red) and internalized CD98 (green) colocalized in tubular endosomes. Shown is a montage of a projection of a 3D image from 0° to 12° with 2° increments. Arrows in C–F point to Hook1 and cargo colocalization positions. Bars: (A–C) 10 µm; (A, insets) 3 µm; (B, insets) 5 µm; (C, inset) 3 µm; (D) 2 µm; (E and F) 1 µm.

To obtain higher-resolution images, we used a wide-field super-resolution imaging system (Gustafsson et al., 2008), the OMX structured illumination microscope. With this microscope we could resolve the endosomal tubules as aligned puncta labeled with the cargo (CD147) in green and Hook1 in red (Fig. 4 C and Video 1). Hook1 can be seen labeling the end of a tubule in box 1 of Fig. 4 C (montage shown in Fig. 4 D and Video 2). Rotation of the volume image in Fig. 4 D confirms that Hook1 decorates the end of the tubule (see Video 2). In another example (Fig. 4 C, box 2; and Fig. 4 E), Hook1 remains associated with one of the cargo puncta associated with the tubule (Video 3). Lastly, imaging of a sample loaded with CD98 antibodies also showed distinct colocalization of Hook1 associated with a tubule containing CD98 cargo (Fig. 4 F and Video 4). Thus, through both conventional confocal microscopy and 3D structured illumination microscopy (SIM), we demonstrate that endogenous Hook1 colocalizes with endosomes containing CD147 and CD98.

Microtubules are required for sorting cargo away from EEA1 compartments

Hook1 can associate with microtubules, and an intact microtubule network is required for the formation of endosomal tubules.

Thus, we wanted to learn whether the binding of Hook1 to microtubules was required for sorting of CD147. In cells treated with nocodazole, a microtubule-depolymerizing agent, the tubules were absent, and internalized CD147 and Hook1 colocalized in scattered endosomal structures (Fig. 5 A). These scattered endosomal structures containing CD147 now colocalized with EEA1 (Fig. 5 B) and to a lesser extent with TfRs (Fig. 5 C). Thus, the absence of microtubules led to a loss of sorting for CD147 with Hook1 associated with endosomes, but unable to connect with microtubules.

Hook1 and Rab22 function together to sort cargo into tubular endosomes

Given that Hook1-Y2H interacts with CD147 by Y2H and coimmunoprecipitation, we asked whether expression of Hook1-Y2H could prevent the binding of endogenous Hook1 to CD147 by acting as a dominant-negative and thus altering trafficking. Strikingly, cells expressing Hook1-Y2H-HA had no tubular endosomes and CD147 was concentrated in punctate structures resembling EEA1-associated endosomes (Fig. 6 A). Although we were unable to localize Hook1, EEA1, and CD147 in the same cells due to antibody limitations, we did look at the distribution of CD147 in Hook1-Y2H–transfected cells lacking tubular endosomes. In those cells, the CD147 localized to endosomal structures labeled with EEA1 (Fig. S2). The failure to load CD147 into the tubules and avoid EEA1 compartments was also observed for CD44 and CD98 (unpublished data). We also noted a decrease in the amount of cargo internalized in many cells. Quantifying the proportion of cells exhibiting tubular endosomes, we found that <10% of the cells expressing Hook1-Y2H showed tubular endosomes. In contrast, almost 100% of control cells contained cargo-loaded tubules (Fig. 6 B). Expression of Hook1-Y2H not only blocked transport to the tubule but also resulted in the loss of tubules as marked by expressed H-Ras (unpublished data), which is present normally on these tubules (Porat-Shliom et al., 2008). These results demonstrate that the carboxyl-terminal sequence of Hook1 can act as a dominant-negative, causing CD147 and other CIE cargo to reach the EEA1 endosomes. Moreover, the data suggest that Hook1 plays a role in maintaining the integrity of the tubular endosomal compartment that has been implicated in CIE cargo recycling (Grant and Donaldson, 2009; Naslavsky and Caplan, 2011).

The loss of tubular endosomes caused by expression of Hook1-Y2H was very similar to the phenotype manifested by cells expressing a dominant-negative Rab22a (Rab22a S19N) that is defective in GTP binding (Weigert et al., 2004). Rab22a activation regulates the recycling of MHCI by controlling the formation of the tubular membranes. Rab22a localizes to tubular recycling endosomes, where it colocalizes with cargo and Arf6 (Weigert et al., 2004). We wondered whether expression of Rab22a could overcome the Hook1 dominant-negative effect and restore the tubular endosomal system. Cells were cotransfected with Hook1-Y2H and GFP-Rab22a, and the distribution of CD147 was analyzed after internalization. Remarkably, overexpression of GFP-Rab22a was sufficient to restore the tubular recycling network in Hook1-Y2H–expressing cells (Fig. 6 A, bottom). Whereas only 5% of cells expressing Hook1-Y2H exhibited tubular endosomes, in cells coexpressing Rab22a this rose to 70%, close to the level observed in untransfected cells (Fig. 6 B). Expression of constitutively active Rab22a also rescued the Hook1-Y2H phenotype, but expression of Rab22a S19N did not (unpublished data). The rescue of Hook1-Y2H

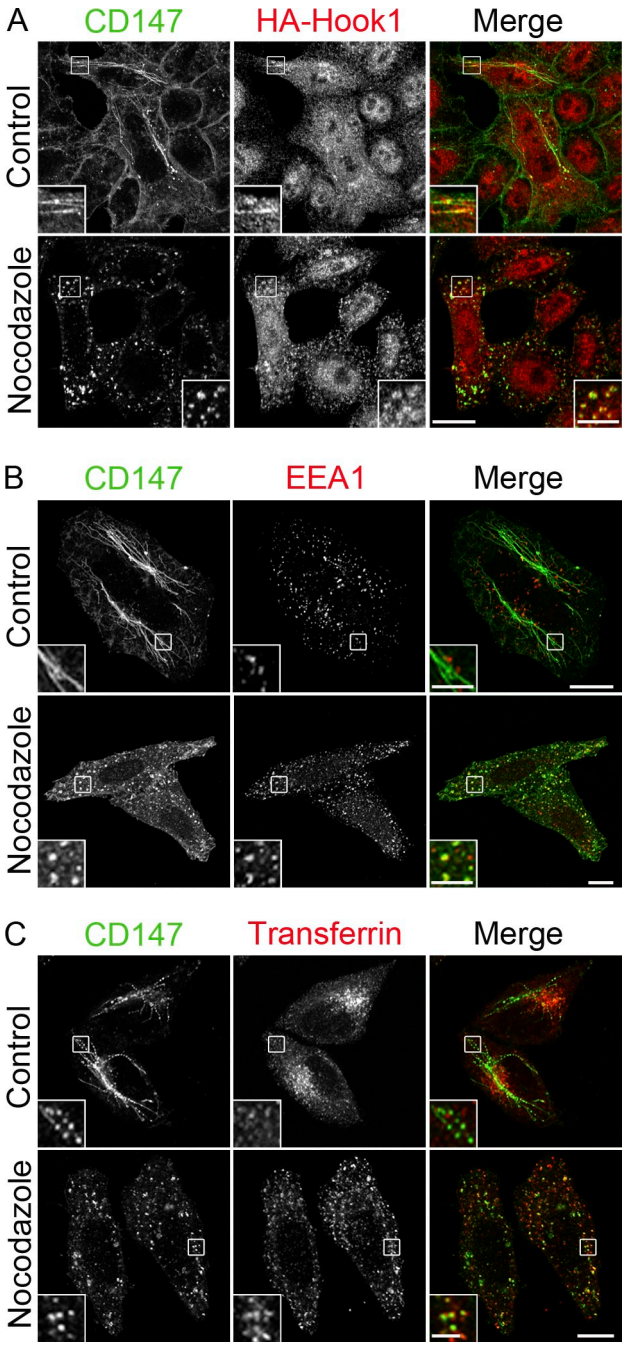

Figure 5. **Endosomal sorting of CD147 requires microtubules.** (A) HeLa cells overexpressing HA-Hook1 were untreated (Control) or pretreated with nocodazole for 2 h at 37°C before anti-CD147 antibody internalization for 30 min. (B) Untransfected HeLa cells were treated as described in A and then fixed and labeled with antibodies to EEA1. (C) Cells were incubated with CD147 antibody and Alexa Fluor 594–conjugated transferrin for 30 min at 37°C in control or nocodazole-containing media. Then the cells were fixed and stained with the respective secondary antibodies. Insets show enlarged views of the boxed panels. Bars: (A–C) 10 µm; (A and B, insets) 5 µm; (C, insets) 3 µm.

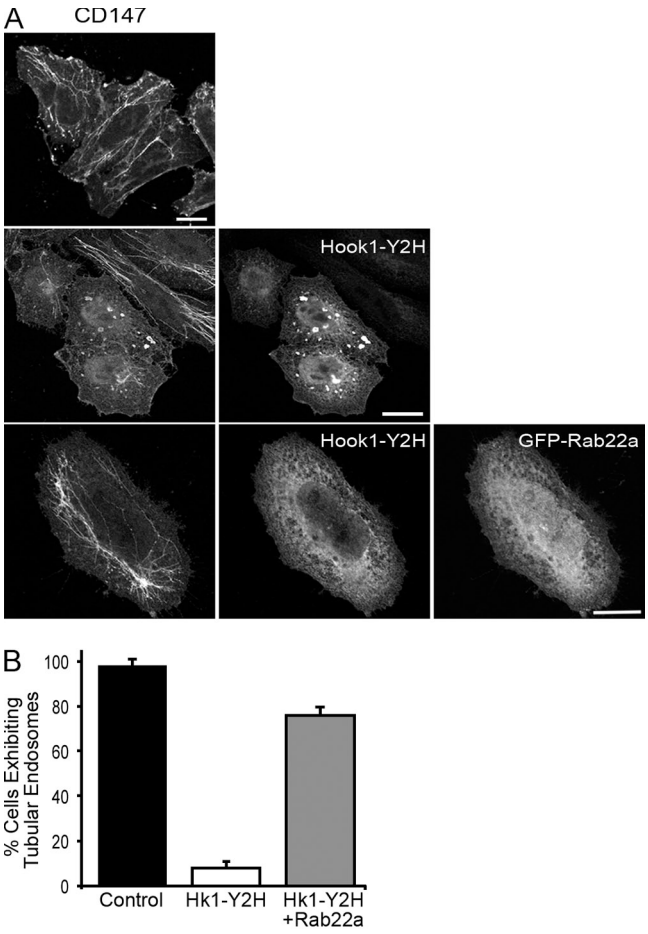

Figure 6. **Expression of Hook1-Y2H results in loss of the recycling tubular endosomal compartment and the targeting of CIE cargo to EEA1-containing endosomes.** (A) HeLa cells expressing endogenous levels of Hook1 (top), overexpressing Hook1-Y2H-HA (middle), or coexpressing Hook1-Y2H-HA and GFP-Rab22a (bottom) were incubated with anti-CD147 antibody for 1 h at 37°C to allow internalization of bound antibodies. Hook1-Y2H was localized using a rabbit anti-HA antibody. (B) The degree of restoration of the tubular endosomal network in Hook1-Y2H–expressing cells by GFP-Rab22a overexpression was determined by calculating the percentage of cells in each population exhibiting tubular endosomes. The data presented is the mean of three independent experiments ± SD (error bars). More than 100 cells were scored for each sample. Bars, 10 µm.

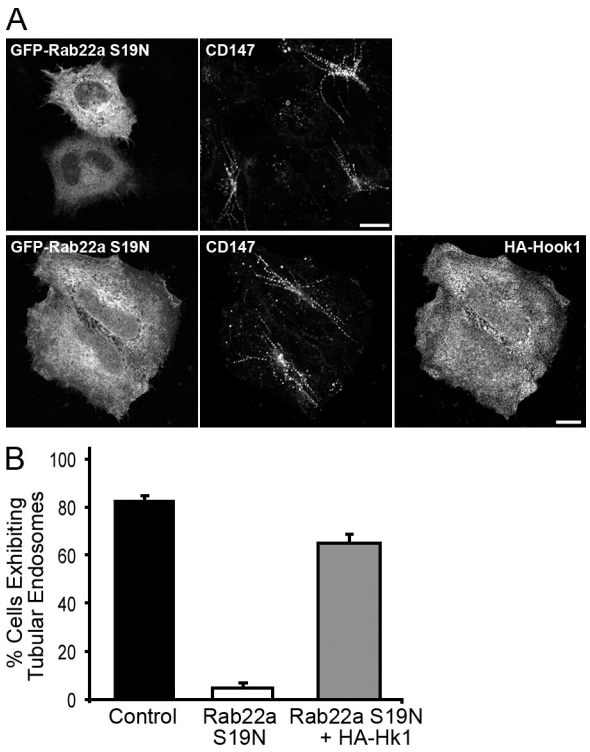

Figure 7. **Hook1 and Rab22a regulate the sorting of CIE cargo proteins into the recycling tubular compartment.** (A) HeLa cells expressing GFP-Rab22a S19N alone or coexpressing GFP-Rab22a S19N and HA-Hook1 were allowed to internalize anti-CD147 antibodies for 30 min at 37°C. HA-Hook1 was visualized using rabbit anti-HA and Alexa Fluor 594–conjugated anti–rabbit antibodies. Bars, 10 µm. (B) Quantitative analysis of the percentage of GFP-Rab22a S19N cells exhibiting tubular endosomes loaded with CD147 in the absence or presence of HA-Hook1. Data presented in the graph are the mean of three independent experiments ± SD (error bars).

with Rab22a was specific, as neither Rab5 nor Rab35 could do this (unpublished data).

Because Rab22a overexpression restored the tubular network in cells expressing Hook-Y2H, we tested whether overexpression of wild-type Hook1 could rescue the loss of recycling tubules observed in cells expressing Rab22 S19N. We transiently cotransfected Rab22a S19N and HA-Hook1 in HeLa cells and then looked at the trafficking itinerary of CD147 in these cells. As described previously (Weigert et al., 2004), in cells expressing only Rab22a S19N, the tubular recycling endosomes were lost and the cargo was observed in small internal punctate structures (Fig. 7 A). However, coexpression of HA-Hook1 led to the restoration of tubular recycling endosomes in nearly 70% of cells and redistribution of CD147 to the tubular endosomes (Fig. 7, A and B). Together, these results suggest that the activities of Rab22a and Hook1 are required at the same step during the segregation of the cargo, potentially in a sorting endosome that is Rab5 positive and EEA1 negative. Rab22a and Hook1 activities may be working in coordination to achieve the successful segregation of the CIE cargo into the recycling route of the pathway.

Depletion of Hook1 or Rab22a inhibits the endosomal sorting of CIE cargo into the tubular recycling endosomes

The fact that Hook1 and Rab22a mutually rescue the phenotypes of their respective dominant-negatives led us to hypothesize that both act during the sorting step and are required for delivery of the cargo to the tubular recycling compartment. Our group has previously demonstrated that siRNA-mediated depletion of Rab22a negatively affects the recycling of CIE cargo and dramatically reduces the formation of tubular recycling endosomes (Weigert et al., 2004). We first examined the effects of Rab22a depletion on the sorting of CIE cargo proteins. Using siRNA in HeLa cells, Rab22a levels were reduced to 13% of that of control cells (Fig. 8 A). The number of cells with tubular endosomes for all CIE cargo proteins was reduced substantially in cells depleted of Rab22a (Fig. 8 B, C and D). Furthermore, CD147 and CD98 were now associated with EEA1-labeled endosomes to similar levels to that of MHCI (Fig. 8 B, C and E). Thus, for all CIE cargo proteins, loss of Rab22a leads to loss of

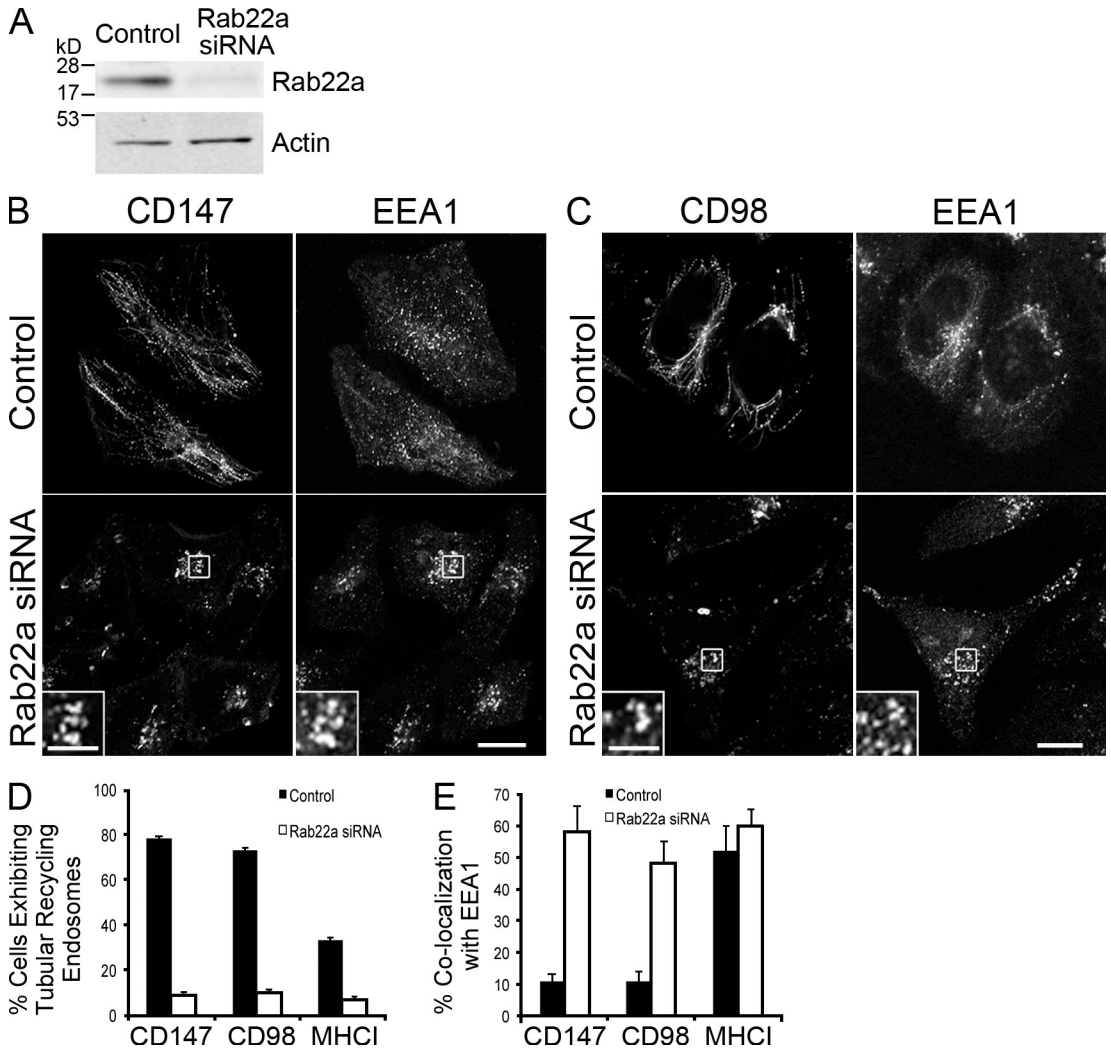

Figure 8. **Depletion of Rab22a affects CIE cargo tubular endosome biogenesis and sorting into EEA1-associated endosomes.** (A) Rab22a protein levels in control or siRNA-treated cells were determined using Western blotting of cell lysates with an antibody against Rab22a and actin (loading control). (B and C) Control- or siRNA-treated cells were allowed to internalize antibody to CD147 and CD98 for 1 h at 37°C and processed for immunofluorescence and confocal microscopy. (D) Control- or siRNA-treated cells were scored for CIE cargo-containing tubules as described in Materials and methods. Results presented in the graph are the means of two independent experiments. (E) Quantitative analysis of colocalization between EEA1 and CIE cargo in control- and siRNA-treated cells. The graph shows the mean and standard deviation for the population of cells (20 cells per condition) from one representative experiment, repeated twice. Bars: (B and C) 10 µm; (B and C, insets) 5 µm.

the tubules associated with recycling and an increased colocalization with EEA1.

Next, we used siRNA directed against Hook1 and were able to reduce levels of Hook1 to 10% of control cells (Fig. 9 A). In Hook1-depleted cells, the percentage of cells showing tubular endosomes loaded with either CD147 (Fig. 9 B) or CD98 (Fig. 9 C) was reduced down to the level that was observed for MHCI-containing tubules (Fig. 9 D) but not to the level observed with Rab22a depletion (Fig. 8 D). However, the depletion of endogenous Hook1 caused a significant increase in the degree of colocalization of CD147 and CD98 with EEA1 close to the level observed for MHCI, which was not significantly affected by depletion of Hook1 (Fig. 9, B, C, and E). The specific effects of Hook1 depletion on the segregation and distribution of CD147 and CD98 suggest that Hook1 functions to sort these proteins directly to the recycling compartment and away from EEA1-associated endosomes.

Depletion of Hook1 inhibits recycling of CD98 and cell spreading

Because the loss of Hook1 resulted in a change in the trafficking itinerary of CD147 and CD98 to one resembling that of MHCI, we wondered whether loss of Hook1 would affect the recycling of CD147, CD98, and MHCI. To do this, we used a fluorescence-based assay used previously (Weigert et al., 2004). In brief, antibodies to CD98 and MHCI and Alexa Fluor 594–conjugated transferrin were allowed to enter cells for 30 min. The surface antibodies were then removed, and reappearance of antibodies back to the cell surface or loss of labeled transferrin was measured after a 30-min recycling period. In control cells, we found that 39% of CD98, 16% of MHCI, and 58% of TfR was recycled back to the PM during this period (Fig. 10 A). In Hook1-depleted cells, the recycling of CD98 was significantly inhibited from 39% to 8%, whereas recycling of MHCI and TfR was not affected (Fig. 10 A).

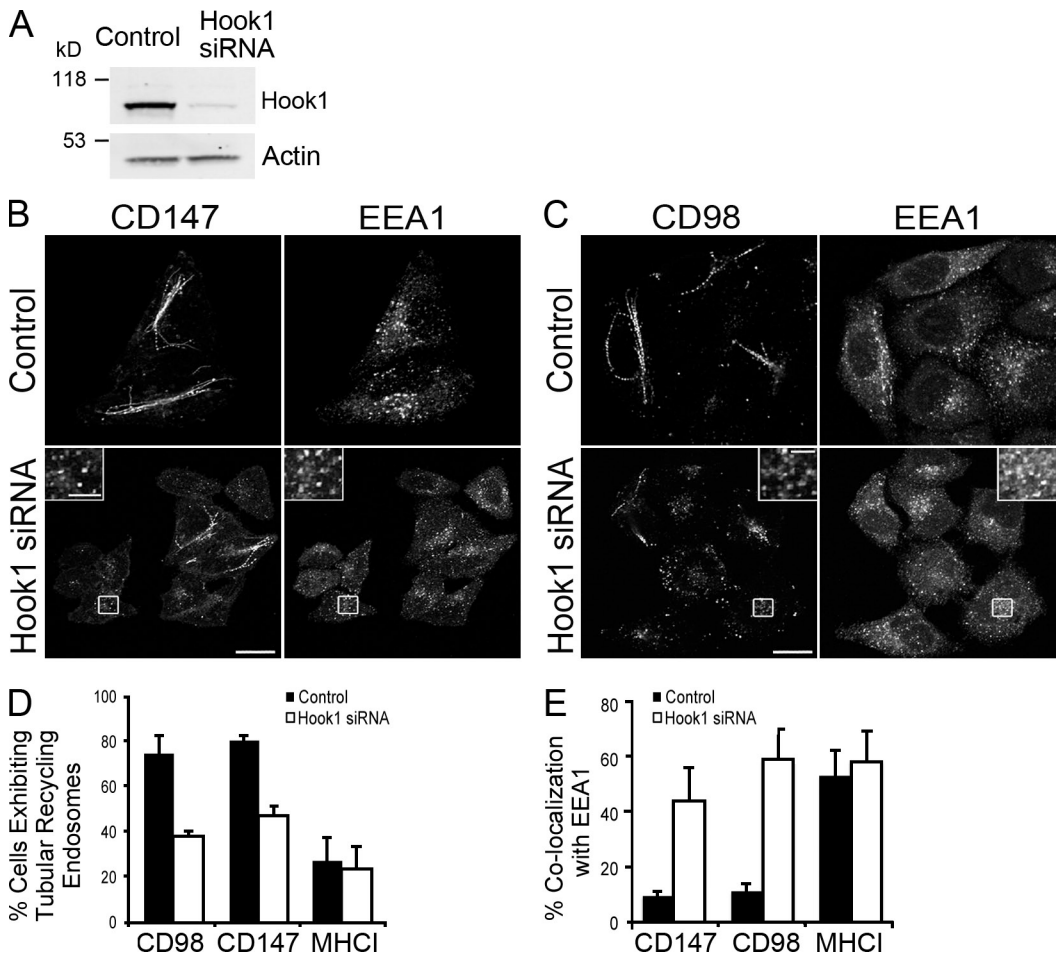

Figure 9. **Depletion of Hook1 affects tubular endosome formation and endosomal sorting of CIE cargo proteins.** HeLa cells were treated with On-TARGET plus SMARTpool siRNA directed against Hook1 as described in Materials and methods. (A) Western blot showing the reduction of Hook1 protein levels in siRNA-treated versus control cells. Hook1 was detected using rabbit anti-Hook1 antibody and Alexa Fluor 680–conjugated anti–rabbit antibody. Actin was used as a loading control. (B and C) Control and Hook1 siRNA-depleted cells were incubated with CD147, CD98, and MHCI antibodies for 1 h at 37°C. After internalization, the cells were fixed and processed for immunofluorescence. Insets show enlarged views of the boxed regions. (D) Quantitative analysis of the percentage of cells exhibiting tubular endosomes loaded with CD147, CD98, and MHCI in control versus Hook1 siRNA-depleted cells. Data presented is the mean of three independent experiments ± SD (error bars). (E) The percentage of colocalization between CIE cargo and EEA1 after Hook1 depletion was determined using MetaMorph software (see Materials and methods). The graphs shows the mean and standard error for the population of cells (error bars; 20 cells per condition) from one experiment, repeated three times. Bars: (B and C) 10 µm; (B and C, insets) 5 µm.

Thus, Hook1 specifically facilitates the sorting and recycling of CD98, and presumably also that of CD44 and CD147.

Previous work demonstrated that membrane recycling of CIE cargo is required for cell spreading in HeLa cells (Song et al., 1998). Upon Arf6 inactivation or expression of the GTP binding–defective mutant of ARF6 T27N, the recycling of internalized membranes is inhibited, resulting in inhibition of cell spreading (Song et al., 1998; Radhakrishna et al., 1999; Balasubramanian et al., 2007). Because the reduction of endogenous Hook1 protein levels redirected CD98 and CD147 to the EEA1-positive endosomes (Fig. 9) and led to an inhibition of recycling of CD98 (Fig. 10 A), we wondered whether Hook1-mediated trafficking of CIE cargo proteins was required for cell spreading. To answer this question, Hook1 siRNA-treated cells were detached from the culture dish and replated onto coverslips for 6 h. The cells were fixed and stained with rhodamine phalloidin to facilitate the visualization and scoring of the phenotype. At 6 h, the control cells were mostly spread, whereas the majority of the siRNA-treated cells were attached but still rounded (Fig. 10 B). We quantified the cells that were spread and found that at 6 h, 60% of control cells were spread, whereas only 27% of the siRNA-treated cells exhibited that phenotype (Fig. 10 C). This finding suggests that it may be the recycling of proteins such as CD44, CD98, and CD147 that is required for cell spreading and that Hook1 facilitates cell spreading through the sorting of these CIE cargo proteins for efficient recycling.

Discussion

CIE is thought to be a nonselective process for internalization of bulk membrane (Hansen and Nichols, 2009; Sandvig et al., 2011). Here we show that after endocytosis of bulk membrane by CIE, some cargo proteins (CD44, CD98, and CD147) are recognized and sorted on endosomes by Hook1, acting with Rab22a, to facilitate rapid routing of this cargo to recycling endosomes, avoiding the default route to EEA1-associated endosomes and lysosomes.

An examination of the cytoplasmic tails of all CIE cargo proteins reveals no common sequence information, which is consistent with the lack of cargo selection at the endocytic step. However, an altered intracellular itinerary is taken by some of these cargo proteins (CD147, CD44, and CD98; Eyster et al., 2009), and in this study we identified cytoplasmic sequences in CD147 and CD44 that were sufficient to redirect the trafficking of Tac, a reporter protein. One feature common to the cytoplasmic tails of CD147, CD44, and CD98 is the presence of acidic amino acid pairs or clusters. In contrast, the cargo that traffics along the default pathway (Tac, MHCI, Glut1, and GPI-APs CD55 and CD59) lacks such di-acidic residues. The acidic residues in CD147 contributed to endosomal sorting in that mutation of these residues led to impaired sorting and lack of interaction in the Y2H screen. However, sorting was not completely lost when the acidic residues were mutated, which suggests that other sequences may contribute to the sorting. A sorting role for a single leucine (at position 248 in the human sequence) in basolateral targeting of CD147 in MDCK cells has been reported (Deora et al., 2004); however, we did not observe altered trafficking of a leucine mutant of CD147 (unpublished data). Acidic clusters have been observed in other PM proteins entering cells by CIE. The inwardly rectifying K channel, Kir3.4, contains clusters of acidic amino acids that were found to be critical for maintaining these channels at the cell surface (Gong et al., 2007). As these proteins become trapped in vacuoles generated by expression of Arf6 Q67L, it is likely that Kir3.4 travels along the CIE pathway, is sorted along with CD147, CD44, and CD98, and might be sorted via Hook1.

The evidence for sorting of proteins on endosomes is increasing and has been observed for those proteins entering by CIE and CME. Distinct cytoplasmic sequences on G protein–coupled receptors promote sorting out of early endosomes to facilitate receptor recycling after ligand-stimulated CME (Puthenveedu et al., 2010). Phenylalanine-containing clusters in the cytoplasmic portion of the TfR may be important for normal rate of recycling of the receptor (Dai et al., 2004). Interestingly, two cargo proteins that enter cells by the CIE pathway described here, CD44 and syndecan 2, both contain carboxyl-terminal PDZ binding motifs. In the case of syndecan 2, the PDZ domain protein syntenin is required for syndecan 2 to recycle back to the surface (Zimmermann et al., 2005). The identification of the machinery that recognizes and sorts these different cargo proteins will likely include roles for sorting nexins, ubiquitin-interacting proteins, and the known Rabs and EHD proteins implicated in various recycling pathways (Grant and Donaldson, 2009; Naslavsky and Caplan, 2011).

We found that Hook1 specifically binds to CD147 and facilitates the microtubule-dependent sorting of CD147, CD44, and CD98 away from EEA1-positive endosomes and into recycling tubules. Hook1 is well suited to perform such a function, as it contains an amino-terminal domain associated with microtubule binding and a carboxyl-terminal domain associated with cargo binding. The Hook protein was originally identified in *Drosophila melanogaster*, where it functions in the trafficking to late endosomes (Krämer and Phistry, 1996; Sunio et al., 1999). There are three mammalian Hook proteins. Hook2 has

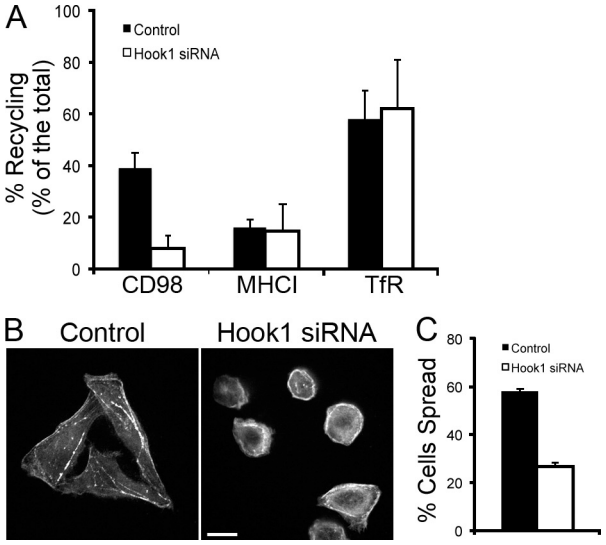

Figure 10. **Hook1 depletion inhibits recycling of CD98 and cell spreading in HeLa cells.** (A) The amount of protein recycled back to the PM for CD98, MHCI, and the TfR in control and Hook1 siRNA-depleted cells was determined using the protocol described in Materials and methods. Cells were incubated with antibodies against CD98 or MCHI, or loaded with Alexa Fluor 594-Tf for 30 min at 37°C. After internalization, remaining surface-bound antibody was removed by a brief acid wash. Then the cells were incubated for 30 min at 37°C to allow recycling. The percentage of recycling for each cargo proteins was calculated, and shown here is the mean recycling from three independent experiments ± SD (error bars). To confirm the statistical significance of the results, the two-tailed Student's *t* test was used. For CD98 recycling, the p-value for control versus Hook1-depleted cells was $P < 0.05$. For MHCI and TfR recycling, the values were not significantly different. (B) Control and Hook1 siRNA-treated cells were detached from the culture dish and replated onto coverslips for 6 h. The cells were fixed and stained with rhodamine phalloidin to facilitate the visualization and scoring of the phenotype. Bar, 10 µm. (C) The percentage of attached cells on the coverslips that were spread was determined by scoring >100 cells. The data shown are the means of "% cells spread" from three independent experiments ± SD (error bars).

been localized to the centrosome (Szebenyi et al., 2007) and Golgi (Baron Gaillard et al., 2011), and has been shown to be involved in the formation of the primary cilium (Baron Gaillard et al., 2011). Hook3 also localizes to the Golgi (Walenta et al., 2001). We found partial colocalization of endogenous Hook1 with CD147 and other CIE cargo proteins in tubular endosomes, and this localization was enhanced in the absence of microtubules. We could detect a biochemical interaction of CD147 and CD98 with the carboxyl-terminal domain of Hook1, but not with the full-length protein. This might be caused by some type of autoinhibitory or regulatory interaction of the full-length protein that we are currently examining in more detail. Two other proteins have been identified that interact with the carboxyl-terminal region of Hook1. These are the Vps18 subunit of the HOPs complex (Richardson et al., 2004) and AKTIP (Xu et al., 2008), an E2 ubiquitin-conjugating enzyme also known as FTS. We do not know whether the interaction of these proteins with Hook1 plays a role in sorting of CD147, but the fact that these proteins may form larger complexes suggests that the Hook1-associated machinery interacting with and sorting CIE cargo proteins might involve other components.

Indeed, another component of the sorting machinery is Rab22a, which we previously showed to be required for the

formation of the recycling endosomal tubules in HeLa cells (Weigert et al., 2004). Here we extend Rab22a function to that of assisting Hook1 in the sorting of CIE cargo (CD44, CD98, and CD147) into the tubules. Hook1 has been shown to coimmunoprecipitate with overexpressed Rab7, Rab9, and Rab11, which suggests that Hook1 might interact with endosomal Rabs (Luiro et al., 2004); however, for Rab22a, we could not see a direct interaction with Hook1. Although we could not detect direct biochemical interaction between Hook1 and Rab22a, these two proteins seem to be acting at the same sorting step in cells, given that each effectively rescued the dominant-negative phenotypes induced by the other. Because dominant-negative proteins often sequester essential components, this striking characteristic for Hook1 and Rab22 suggests that they may be interacting with additional components to relieve the mutant phenotypes. Rab22a has been implicated in TfR recycling in other cells (Magadán et al., 2006) and in preventing phagosome maturation in cells harboring mycobacteria (Roberts et al., 2006), a phenotype of lysosome avoidance that is consistent with observations reported here. A similar coordination between a Hook and a Rab has been observed in that Rab8 overexpression suppresses the effect of Hook2 knockdown on ciliogenesis (Baron Gaillard et al., 2011). Given the microtubule dependence of cargo sorting and the connection of Hook1 with microtubules, it is likely that Hook1 and Rab22a act together with a microtubule motor protein such as a kinesin or dynein (Horgan and McCaffrey, 2011).

This sorting at the level of the endosome provides a means to monitor protein quality control of cell surface proteins. By sampling the PM by bulk endocytosis, PM proteins can be monitored and sorted, allowing some proteins to recycle back out to the PM, and for misfolded or malfunctioning, ubiquitinated cargo to be sent on to degradation. Further investigations will identify additional signals that can influence this sorting; e.g., how ubiquitination of CIE cargo proteins could affect their sorting on endosomes.

The proteins that are directly sorted into recycling tubules, CD44, CD98, and CD147, are all implicated in cell–cell and cell–matrix interactions. As such, they may be important cell surface components that influence cell adhesion and migratory properties, and as we observed here are important for cell spreading. CD44 is a hyaluronan receptor (Zöller, 2011) and can influence growth factor signaling (Ponta et al., 2003). CD98 plays an important role in nutrient uptake through its association with amino acid transporters (Yan et al., 2008), and interacts with and influences integrin trafficking and signaling (Cantor and Ginsberg, 2012). CD147, also known as Basigin or EMMPRIN (extracellular matrix metalloproteinase inducer) associates with integrins and monocarboxylate transporters, and interacts with matrix metalloproteases (Iacono et al., 2007). Levels of CD44, CD98, and CD147 are elevated in many cancers, which suggests that the rapid recycling and avoidance of degradation observed here could contribute to this phenotype. The ability of cells to segregate and rapidly recycle these proteins might be carefully regulated in tissues during development and turned on during wound healing and cancer cell metastasis. Identifying additional sorting components and understanding the mechanism of how these proteins are sorted on endosomes could lead to novel therapeutic targets.

Materials and methods

Cells, reagents, and antibodies

HeLa cells were cultured in DMEM (Lonza) with 10% fetal bovine serum, 2 mM glutamine, 100 U/ml penicillin, and 100 µg/ml streptomycin and grown in a 5% CO_2 atmosphere at 37°C. Nocodazole, saponin, and digitonin were from Sigma-Aldrich. BG-PEG_4-biotin was synthesized by conjugating a 1:1 molar ratio of BG-NH2 (Toronto Research Chemicals) with NHS-PEG_4-biotin (Thermo Fisher Scientific) in dimethylformamide and a threefold molar excess of triethylamine for 16 h at 30°C. Analysis of the product (m/z 744.4) was performed on an high-pressure liquid chromatograph (1100 series; Agilent Technologies) with electrospray ionization and detected by a mass spectrometer (model G1946) equipped with a time-of-flight detector (Agilent Technologies).

Mouse monoclonal antibodies to human CD147 (clone HIM6; IgG1), human CD98 (clone MEM-108; IgG1), and human CD44 (clone BJ18; IgG1) were from BioLegend and used at a 1:250 dilution for antibody internalization experiments. Mouse monoclonal antibodies to rat CD147 (clone OX-47; IgG1) were used to look at the distribution of the CD147-Tac chimera at a 1:100 dilution (BioLegend). Mouse monoclonal antibodies to human MHCI (clone W6/32; IgG2a) were used in antibody uptake experiments at a 1:100 dilution (BioLegend). Culture supernatants from a hybridoma cell line for mouse anti-Tac (clone 7G7B6; IgG2a) diluted 1:5 were used in immunofluorescence and antibody uptake experiments (Naslavsky et al., 2003). The rabbit polyclonal antibody anti–human Rab22a was raised against the carboxyl terminus of human Rab22a (1:500 dilution for immunoblotting; Weigert et al., 2004). A rabbit polyclonal anti–human Hook1 directed against the carboxyl terminus of Hook1 was used to detect the protein by immunoblotting (1:2,000) and immunofluorescence (1:1,000; Walenta et al., 2001). Rabbit anti-EEA1 and rabbit anti-Lamp1 were purchased from BD and Abcam, respectively. Rabbit antibodies to HA (clone 16B12; 1:1,000) were from Covance. Rabbit anti-actin antibodies were from Sigma-Aldrich (clone A 2066; 1:5,000). All secondary antibodies (Alexa Fluor 488–conjugated goat anti–mouse, Alexa Fluor 594–conjugated goat anti–mouse and goat anti–rabbit, Alexa Fluor 633–conjugated goat anti–rabbit, and Alexa Fluor 568–conjugated goat anti–rabbit) were used at a dilution of 1:500 (Invitrogen). Transferrin conjugated to Alexa Fluor 594 was purchased from Invitrogen and used at a 1:1,000 dilution in internalization assays.

Plasmids and transient transfections

All chimeras were in the cytomegalovirus promoter-driven mammalian expression vector pTarget (Promega). CD44-Tac was constructed by two-stage PCR with overlapping CD44 and Tac-specific oligos. These fused the luminal domain of human *CD44* (AAH04372) with the TM domain and cytoplasmic sequence of Tac (TPQIPEWVAVAGCV . . . SRRTI). CD147-Tac was constructed by two-stage PCR with overlapping CD147 and Tac-specific oligos. These fused the luminal domain of rat *CD147* isoform 2 (available from GenBank under accession no. NM_198589; provided by E. Rodriguez-Boulan, Weill Medical College of Cornell University, New York, NY) with the TM domain and cytoplasmic tail of Tac (RVRSRLVAVAGCV . . . SSRTI). The luminal domain of rat CD147 isoform 2 was used to distinguish the CD147-Tac chimera from endogenous CD147. The Tac-CD44 was constructed by two-stage PCR with overlapping Tac- and CD44-specific oligos. The designed oligos fused the luminal domain of *Tac* with the TM domain and cytoplasmic tail of CD44 (SIFTTVYQLIILASL . . . MKIGV). Tac-CD147 was constructed by two-stage PCR with overlapping Tac- and CD147-specific oligos. The oligos were designed to fuse the luminal domain of the α chain of the interleukin 2 receptor *Tac* (accession no. NM_000417) with the TM domain and cytoplasmic sequence of human CD147 (accession no. NM_198589; SIFTTEAALWPFL . . . NVRQRNSS).

For SNAP-CD147, the signal peptide for hen egg lysozyme (MRSLLILVLCFLPLAALG) was introduced just before the second amino acid of the SNAP tag (DKDCEMKR . . .). Following the SNAP-tag, a $(GGGGS)_2$ linker was introduced, followed by the extracellular, TM, and cytoplasmic tail domains of isoform 2 of human CD147 (accession no. NM_198589; AAGTVFTTVED . . . NVRQRNSS). This construct was cloned into the mammalian expression vector pcDNA3.1 and generated by standard PCR and cloning techniques. CD98-SNAP was constructed by fusing the SNAP

open reading frame (pSEMS1-26m from New England Biolabs, Inc.) onto the carboxyl terminus of the type-II protein CD98 (4F2 cell-surface antigen heavy-chain isoform b) by standard two-stage PCR protocols. CD98 was separated from the SNAP-tag by a $(GGGS)_2$ linker (. . . GLLLRFPYAAGGGGSGGGGSDKDCEMKRT . . .). The PCR fusion was cloned into the TA mammalian expression vector pTarget (Promega; Eyster et al., 2011).

The Hook1-Y2H-HA plasmid was constructed by using specific oligos to amplify the sequence encoding for amino acids 486–728 of human Hook1 using an HA-Hook1 construct as a template (Krämer and Phistry, 1999). Hook1-Y2H-HA was cloned into the mammalian expression vector pcDNA3.1. Standard PCR and cloning techniques were used in the preparation of this construct.

The human Rab22a cDNA clone (accession no. NM_020673) was purchased from OriGene and was subcloned into the SalI–BamHI sites of pEGFP-C3 (BD/Clontech) to generate the GFP-Rab22a construct. All amino acid substitutions in the GFP-Rab22a construct and various chimeras were made using specific oligos harboring the mutations of interest and the QuikChange Lightning site-directed mutagenesis kit (Agilent Technologies) according to the manufacturer's instructions. All restriction enzymes were purchased from New England Biolabs, Inc.

HeLa cells were grown on glass coverslips (for immunofluorescence experiments), 35-cm dishes (for siRNA depletion assays), and 10-cm plates (for immunoprecipitation and Western blotting). Cells were transiently transfected using Fugene 6 according to the manufacturer's instructions (Roche). Experiments were performed 15–18 h after transfection.

siRNA interference

Hook1 siRNA depletion was achieved by using the ON-TARGETplus SMARTpool human Hook1 siRNA (accession no. NM_015888) from Thermo Fisher Scientific. The siRNA was prepared according to manufacturer's instructions, and cells were transfected with Lipofectamine 2000 (Invitrogen). After 48 h of transfection, cells were trypsinized, diluted 1:10, and seeded in 35-mm dishes. Cells were incubated in antibiotic-free media for 24 h. Then, the second treatment was applied to the cells for additional 48 h. Next, cells were trypsinized and seeded in 10-cm dishes with coverslips and used for experiments the following day. Human Rab22a siRNA depletion was performed using the ON-TARGETplus SMARTpool human Rab22a siRNA (accession no. NM_020673) from Thermo Fisher Scientific. Cells were treated as described for Hook1 siRNA, with the exception that after the second transfection we waited 72 h to trypsinize the cells (Weigert et al., 2004).

Antibody internalization, immunofluorescence, and confocal analysis

Antibody internalization assays were performed as described previously (Eyster et al., 2009). In brief, cells were incubated with primary antibodies against endogenous CIE cargo proteins (CD44, CD98, CD147, and MHCI) or Tac for 30 min or 1 h at 37°C to allow internalization of the antibody-bound cargo proteins. After antibody internalization, cells were rinsed twice with PBS, and MHCI and CD98 surface antibodies were removed by rinsing the cells in low-pH solution (0.5% acetic acid and 0.5 M NaCl, pH 3.0) for 30 s, followed by two rinses with PBS. Then, cells were fixed in 2% formaldehyde in PBS for 10 min at room temperature. After fixation, cells were rinsed two times with PBS (5-min washes). Remaining PM CD44, CD147, and Tac-associated antibodies were blocked by incubating fixed cells with unlabeled goat anti–mouse IgG (1:20; Jackson ImmunoResearch Laboratories, Inc.) for 1 h in the absence of saponin. Internalized antibodies were then visualized by incubating the cells for 30 min at room temperature with Alexa Fluor–conjugated secondary antibodies (Alexa Fluor 488, Alexa Fluor 594, Alexa Fluor 568, and Alexa Fluor 633; Invitrogen) in PBS buffer containing 10% fetal calf serum and 0.1% saponin. Coverslips were washed two times with PBS buffer containing 10% fetal calf serum and were submitted to a final wash with only PBS. Each wash was done for 5 min. Then coverslips were mounted on glass slides using Fluromount-G as mounting media (SouthernBiotech).

For antibody internalization and NH_4Cl chase experiments, the cells were preincubated with primary antibodies for 30 min or 1 h at 37°C. Cells were transferred to fresh media containing 15 mM NH_4Cl for 22 h. After 22 h, the cells were rinse in PBS and processed for immunofluorescence as described in the previous paragraph (Eyster et al., 2011).

Hook1 was visualized using a rabbit polyclonal antibody (Walenta et al., 2001). Before fixation, cells were treated for 1 min with 10 µg/ml digitonin on ice, followed by two rinses with PBS. Then, cells were fixed and processed for immunofluorescence as described in the previous paragraph.

All images were obtained at room temperature using a confocal microscope (LSM 510; Carl Zeiss) with a 63× 1.4 NA Plan-Apochromat oil immersion objective lens and 488-, 532-, and 633-nm laser excitation. Images were acquired using the LSM 510 software (Carl Zeiss) and processed using Photoshop CS4 (Adobe). The MetaMorph colocalization application (Molecular Devices) was used to quantify colocalization between EEA1 and the CIE cargo proteins in individual cells. After separating the confocal images in the two different colors, individual cells were outlined using the MetaMorph trace region tool. After thresholding, quantification of the amount of overlapping fluorescence pixels per cell was obtained after applying the colocalization function. Data analysis was done using the Excel software (Eyster et al., 2011). To score the percentage of cells exhibiting CIE cargo-containing tubules after CIE cargo internalization under several conditions, we followed the protocol described in Weigert et al. (2004). In brief, 100 cells or more (two coverslips per experiment/condition) were scored (cells with tubes or cells without tubes) per condition using an epifluorescence photomicroscope (Carl Zeiss) with a 63×/1.4 NA Plan-Apochromat oil immersion objective lens using either the 488 channel or the 594 channel depending on the Alexa Fluor–conjugated secondary antibody used. The results are means of three independent experiments ± SD. Excel software was used to generate all the bar graphs and statistical analysis of the data. All the figures were produced using Photoshop CS4.

3D SIM

Super-resolution fluorescence microscopy was performed using an imaging system in 3D SIM mode (DeltaVision OMX V4; Applied Precision/GE). Images were taken with a Plan-Apochromat N 60× 1.42 NA oil objective lens (Olympus) at room temperature. The excitation lasers of 488 nm and 568 nm (100 mW for both lasers) were attenuated to 10% transmission. The exposure times were 25 ms and 80 ms for 488 nm and 568 nm, respectively. Stacks of 41 z sections were taken over a cell thickness of 5 µm at a spacing of every 125 nm. The microscope is calibrated before experiments to calculate both the lateral and axial limits of image resolution under our experimental conditions. All raw images were processed and reconstructed in 3D using DV SoftWoRx software (Applied Precision/GE). 3D images are presented with projections from 0° to 60° in 2° increments. Montages of the super-resolution images were produced using MetaMorph software (Molecular Devices).

Recycling assay for CD98, MHCI, and transferrin

Recycling of CD98, MHCI, and transferrin was measured in control and Hook1 siRNA-depleted HeLa cells using the fluorescence-based assay described previously (Weigert et al., 2004). Cells grown on glass coverslips were incubated with primary antibodies against CD98, MCHI, or with Alexa Fluor 594–conjugated transferrin for 30 min at 37°C. In the case of transferrin, cells were serum starved for 30 min at 37°C prior to incubation with Alexa Fluor 594–conjugated transferrin. After internalization, the cells were rinsed twice with PBS and treated with acidic buffer (0.5% acetic acid and 0.5 M NaCl, pH 3.0) for 20 s to remove surface-bound antibody that was not internalized. The acid stripping of the surface-bound antibody was followed by two rinses with PBS and two rinses with complete DMEM. To obtain the time 0 data, a set of coverslips was fixed immediately after the washing steps. The rest of the cells were returned to the incubator (37°C) for 30 min in complete medium to allow for the recycling of CD98, MHCI, and transferrin. After the 30 min of incubation, cells were fixed in PBS/2% formaldehyde for 10 min, and the surface pools of CD98 and MHCI were detected using goat anti–mouse IgG Alexa Fluor 594–conjugated antibody. Another subset of coverslips were washed with low pH buffer, fixed, and stained with goat anti–mouse IgG Alexa Fluor 594–conjugated antibody in the presence of 0.1% saponin. To determine the amount of cargo at the surface or inside the cell, we analyzed 60–70 cells (sizes between 500 and 1,500 μm^2) using a confocal microscope (LSM 780; Carl Zeiss) with a 63×/NA 1.4 Plan-Apochromat oil immersion objective lens. The cells were imaged using the same acquisition parameters (room temperature, pinhole completely open, fluorescence signal in the dynamic range, etc.), which were set up using the time 0 coverslip, revealing the internal pool. The total internal and surface florescence for each time point was determined using MetaMorph software. The total surface or internal fluorescence per cell was obtained using the integrated intensity-measuring application tool without threshold. The amount of cargo recycled after 30 min was obtained by expressing the surface fluorescence as a percentage of the total fluorescence (sum of the internal and the surface fluorescence) for each cargo. Final measurements were obtained after subtracting the background signal, which was the amount remaining at the surface at time 0. Excel software (Microsoft) was used to process the data collected, generate the bar graphs, and perform statistical analysis.

Nocodazole treatment and replating for the cell-spreading assay

HeLa cells grown on coverslips were pretreated with 10 µg/ml nocodazole for 2 h at 37°C. Control cells were pretreated for 2 h with DMSO. Then cells were incubated with primary antibodies against CD147 or with Alexa Fluor 594–conjugated transferrin diluted in media containing either DMSO or nocodazole for 1 h to allow internalization of the antibodies. After internalization, the cells were processed for immunofluorescence as described in the immunofluorescence section.

The cell-spreading assay was performed as described previously (Song et al., 1998). In brief, siRNA-treated and control cells were trypsinized, diluted with culture medium to neutralize the trypsin, and pelleted (300 *g* for 5 min at 4°C). Then cells were washed once with fresh media, pelleted, and resuspended in complete media. A fraction of the suspended cells was added to 10-cm dishes with glass coverslips. At different time points, coverslips were removed, fixed in PBS/2% formaldehyde for 10 min, and stained with rhodamine-phalloidin (Invitrogen). Cells were classified as spread when cells were flattened (at least twice the diameter of the nucleus) and exhibited protrusions. Cells were scored using an epifluorescence photomicroscope (Carl Zeiss) with a 63×/NA 1.4 Plan-Apochromat oil immersion objective lens using either the 594-nm channel. The results are means of three independent experiments ± SD and were calculated using Excel software.

Y2H assays

The Y2H screen was performed using the Matchmaker Gold Yeast Two-Hybrid System (Takara Bio Inc.) and a Mate and Plate Library, Human Universal Normalized CDNA library (Takara Bio Inc.). The screen was performed following the recommendations and instructions of the manufacturer. The Gal4 DNA-BD/bait construct was prepared by ligating the CD147 C-terminal PCR fragment (aa 229–269, accession no. NM_198589) into the BamHI–EcoRI sites of the pGBKT7 vector (TRP1; Takara Bio Inc.) using the In-Fusion Advantage PCR Cloning kit (Takara Bio Inc.). The yeast strain Y2HGold (Takara Bio Inc.) was maintained on YPD agar plates (rich media) or on SD –TRP (tryptophan) plates when transfected with the Gal4 DNA-BD/CD147 bait construct. To confirm the expression of the bait and prey plasmids, the cells were grown on SD-Leu/−TRP plates. The library was transformed into the Y187 yeast strain (Takara Bio Inc.). The Y2H screen was performed under high-stringency growth conditions as recommended by the manufacturer. Yeast cells coexpressing CD147 carboxyl-terminal tail or the CD147 carboxyl-terminal acidic-cluster mutant fused to the GAL4 AD (baits) and the C-terminal sequence of Hook1 or the pGBKT7 empty vector (prey) were grown on plates lacking leucine, tryptophan, histidine, and adenine (−Leu, −Trp, −His, and −Ade) and supplemented with 125 ng/ml Aureobasidin A (high-stringency conditions). Low-stringency growth conditions (−Leu, −Trp, −His, and −Ade without Aureobasidin A) were used to test the interaction between the CD147 carboxyl-terminal acidic-cluster mutant bait and Hook1. Transformations were performed according to the Clontech's Yeast Protocols Handbook (Takara Bio Inc.).

Coimmunoprecipitation and Western blotting

HeLa cells were transiently transfected with equal amounts of DNA encoding the indicated SNAP constructs and Hook1 Y2H clone (aa 486–728 containing a carboxyl-terminal HA tag). After 16 h, cells were labeled with 5 µM of cell-impermeable BG-PEG_4-biotin for 30 min to 2 h at 37°C. Cells were washed three times with PBS, then solubilized in lysis buffer (50 mM Tris-Cl, pH 7.4, 150 mM NaCl, and 1% Triton X-100) containing protease inhibitors (Roche) plus 20 µM BG-NH_2 to block further SNAP labeling. Cell lysates were centrifuged at 13,000 *g* for 5 min, and the soluble fraction was incubated with Streptavidin-agarose beads (GE Healthcare) for 1 h at 4°C. Beads were washed three times with PBS, then heated in sample buffer before bead eluates were run on SDS-PAGE. Proteins were transferred to nitrocellulose and immunoblotted for Hook1 and biotinylated SNAP proteins with rabbit anti-Hook1 antibody (1:2,000) and Alexa Fluor 800–conjugated goat anti–rabbit IgG (Invitrogen), and DyLight 680-conjugated NeutrAvidin (Thermo Fisher Scientific), respectively.

Online supplemental material

Fig. S1 demonstrates that the conserved acidic clusters in the carboxyl terminal of CD147 play a role in the endosomal sorting of CD147 away from EEA1-associted endosomes. Fig. S2 shows that overexpression of the Hook1 Y2H clone results in the redistribution of CD147 into EEA1-associated endosomes. Video 1 shows that endogenous CD147 and Hook1 colocalize on tubular endosomes and endosomal structures. Video 2 shows the localization of endogenous Hook1 at the end of tubular endosome loaded with CD147. Video 3 shows that CD147 and Hook1 colocalize on endosomes. Video 4 shows that endogenous CD98 and endogenous Hook1 colocalize in tubular endosomes. Online supplemental material is available at http://www.jcb.org/cgi/content/full/jcb.201208172/DC1.

We thank E. Rodriguez-Boulan for the rat CD147 expression plasmid. We also thank L. Greene (National Heart, Lung, and Blood Institute [NHLBI]), R. Weigert (National Institute of Dental and Craniofacial Research), R.C. Aguilar (Purdue University), and members of the Donaldson laboratory for discussion and comments on the manuscript. Microscopes used in this study are part of the NHLBI Light Microscopy Core. Special thanks to X. Wu for help in using the OMX microscope (NHLBI Light Microscopy Core).

This work was supported by the Intramural Research Program in the National Heart, Lung, and Blood Institute at the National Institutes of Health (HL006060) and a grant from the National Eye Institute (EY10199) to H. Krämer.

Submitted: 30 August 2012
Accepted: 19 March 2013

References

Balasubramanian, N., D.W. Scott, J.D. Castle, J.E. Casanova, and M.A. Schwartz. 2007. Arf6 and microtubules in adhesion-dependent trafficking of lipid rafts. *Nat. Cell Biol.* 9:1381–1391. http://dx.doi.org/10.1038/ncb1657

Balklava, Z., S. Pant, H. Fares, and B.D. Grant. 2007. Genome-wide analysis identifies a general requirement for polarity proteins in endocytic traffic. *Nat. Cell Biol.* 9:1066–1073. http://dx.doi.org/10.1038/ncb1627

Baron Gaillard, C.L., E. Pallesi-Pocachard, D. Massey-Harroche, F. Richard, J.P. Arsanto, J.P. Chauvin, P. Lecine, H. Krämer, J.P. Borg, and A. Le Bivic. 2011. Hook2 is involved in the morphogenesis of the primary cilium. *Mol. Biol. Cell.* 22:4549–4562. http://dx.doi.org/10.1091/mbc.E11-05-0405

Barral, D.C., M. Cavallari, P.J. McCormick, S. Garg, A.I. Magee, J.S. Bonifacino, G. De Libero, and M.B. Brenner. 2008. CD1a and MHC class I follow a similar endocytic recycling pathway. *Traffic*. 9:1446–1457. http://dx.doi.org/10.1111/j.1600-0854.2008.00781.x

Cantor, J.M., and M.H. Ginsberg. 2012. CD98 at the crossroads of adaptive immunity and cancer. *J. Cell Sci.* 125:1373–1382. http://dx.doi.org/10.1242/jcs.096040

Conner, S.D., and S.L. Schmid. 2003. Regulated portals of entry into the cell. *Nature*. 422:37–44. http://dx.doi.org/10.1038/nature01451

Dai, J., J. Li, E. Bos, M. Porcionatto, R.T. Premont, S. Bourgoin, P.J. Peters, and V.W. Hsu. 2004. ACAP1 promotes endocytic recycling by recognizing recycling sorting signals. *Dev. Cell*. 7:771–776. http://dx.doi.org/10.1016/j.devcel.2004.10.002

Deora, A.A., D. Gravotta, G. Kreitzer, J. Hu, D. Bok, and E. Rodriguez-Boulan. 2004. The basolateral targeting signal of CD147 (EMMPRIN) consists of a single leucine and is not recognized by retinal pigment epithelium. *Mol. Biol. Cell*. 15:4148–4165. http://dx.doi.org/10.1091/mbc.E04-01-0058

Donaldson, J.G., N. Porat-Shliom, and L.A. Cohen. 2009. Clathrin-independent endocytosis: a unique platform for cell signaling and PM remodeling. *Cell. Signal.* 21:1–6. http://dx.doi.org/10.1016/j.cellsig.2008.06.020

Eyster, C.A., J.D. Higginson, R. Huebner, N. Porat-Shliom, R. Weigert, W.W. Wu, R.F. Shen, and J.G. Donaldson. 2009. Discovery of new cargo proteins that enter cells through clathrin-independent endocytosis. *Traffic*. 10:590–599. http://dx.doi.org/10.1111/j.1600-0854.2009.00894.x

Eyster, C.A., N.B. Cole, S. Petersen, K. Viswanathan, K. Früh, and J.G. Donaldson. 2011. MARCH ubiquitin ligases alter the itinerary of clathrin-independent cargo from recycling to degradation. *Mol. Biol. Cell*. 22:3218–3230. http://dx.doi.org/10.1091/mbc.E10-11-0874

Gong, Q., M. Weide, C. Huntsman, Z. Xu, L.Y. Jan, and D. Ma. 2007. Identification and characterization of a new class of trafficking motifs for controlling clathrin-independent internalization and recycling. *J. Biol. Chem.* 282:13087–13097. http://dx.doi.org/10.1074/jbc.M700767200

Grant, B.D., and J.G. Donaldson. 2009. Pathways and mechanisms of endocytic recycling. *Nat. Rev. Mol. Cell Biol.* 10:597–608. http://dx.doi.org/10.1038/nrm2755

Gustafsson, M.G., L. Shao, P.M. Carlton, C.J. Wang, I.N. Golubovskaya, W.Z. Cande, D.A. Agard, and J.W. Sedat. 2008. Three-dimensional resolution doubling in wide-field fluorescence microscopy by structured illumination. *Biophys. J.* 94:4957–4970. http://dx.doi.org/10.1529/biophysj.107.120345

Hansen, C.G., and B.J. Nichols. 2009. Molecular mechanisms of clathrin-independent endocytosis. *J. Cell Sci.* 122:1713–1721. http://dx.doi.org/10.1242/jcs.033951

Hashimoto, S., Y. Onodera, A. Hashimoto, M. Tanaka, M. Hamaguchi, A. Yamada, and H. Sabe. 2004. Requirement for Arf6 in breast cancer invasive activities. *Proc. Natl. Acad. Sci. USA*. 101:6647–6652. http://dx.doi.org/10.1073/pnas.0401753101

Horgan, C.P., and M.W. McCaffrey. 2011. Rab GTPases and microtubule motors. *Biochem. Soc. Trans.* 39:1202–1206. http://dx.doi.org/10.1042/BST0391202

Howes, M.T., M. Kirkham, J. Riches, K. Cortese, P.J. Walser, F. Simpson, M.M. Hill, A. Jones, R. Lundmark, M.R. Lindsay, et al. 2010a. Clathrin-independent carriers form a high capacity endocytic sorting system at the leading edge of migrating cells. *J. Cell Biol.* 190:675–691. http://dx.doi.org/10.1083/jcb.201002119

Howes, M.T., S. Mayor, and R.G. Parton. 2010b. Molecules, mechanisms, and cellular roles of clathrin-independent endocytosis. *Curr. Opin. Cell Biol.* 22:519–527. http://dx.doi.org/10.1016/j.ceb.2010.04.001

Iacono, K.T., A.L. Brown, M.I. Greene, and S.J. Saouaf. 2007. CD147 immunoglobulin superfamily receptor function and role in pathology. *Exp. Mol. Pathol.* 83:283–295. http://dx.doi.org/10.1016/j.yexmp.2007.08.014

Karacsonyi, C., A.S. Miguel, and R. Puertollano. 2007. Mucolipin-2 localizes to the Arf6-associated pathway and regulates recycling of GPI-APs. *Traffic*. 8:1404–1414. http://dx.doi.org/10.1111/j.1600-0854.2007.00619.x

Krämer, H., and M. Phistry. 1996. Mutations in the *Drosophila* hook gene inhibit endocytosis of the boss transmembrane ligand into multivesicular bodies. *J. Cell Biol.* 133:1205–1215. http://dx.doi.org/10.1083/jcb.133.6.1205

Krämer, H., and M. Phistry. 1999. Genetic analysis of hook, a gene required for endocytic trafficking in *drosophila*. *Genetics*. 151:675–684.

Leonard, D., A. Hayakawa, D. Lawe, D. Lambright, K.D. Bellve, C. Standley, L.M. Lifshitz, K.E. Fogarty, and S. Corvera. 2008. Sorting of EGF and transferrin at the plasma membrane and by cargo-specific signaling to EEA1-enriched endosomes. *J. Cell Sci.* 121:3445–3458. http://dx.doi.org/10.1242/jcs.031484

Luiro, K., K. Yliannala, L. Ahtiainen, H. Maunu, I. Järvelä, A. Kyttälä, and A. Jalanko. 2004. Interconnections of CLN3, Hook1 and Rab proteins link Batten disease to defects in the endocytic pathway. *Hum. Mol. Genet.* 13:3017–3027. http://dx.doi.org/10.1093/hmg/ddh321

Magadán, J.G., M.A. Barbieri, R. Mesa, P.D. Stahl, and L.S. Mayorga. 2006. Rab22a regulates the sorting of transferrin to recycling endosomes. *Mol. Cell. Biol.* 26:2595–2614. http://dx.doi.org/10.1128/MCB.26.7.2595-2614.2006

Mayor, S., and R.E. Pagano. 2007. Pathways of clathrin-independent endocytosis. *Nat. Rev. Mol. Cell Biol.* 8:603–612. http://dx.doi.org/10.1038/nrm2216

Naslavsky, N., and S. Caplan. 2011. EHD proteins: key conductors of endocytic transport. *Trends Cell Biol.* 21:122–131. http://dx.doi.org/10.1016/j.tcb.2010.10.003

Naslavsky, N., R. Weigert, and J.G. Donaldson. 2003. Convergence of non-clathrin- and clathrin-derived endosomes involves Arf6 inactivation and changes in phosphoinositides. *Mol. Biol. Cell*. 14:417–431. http://dx.doi.org/10.1091/mbc.02-04-0053

Naslavsky, N., R. Weigert, and J.G. Donaldson. 2004. Characterization of a nonclathrin endocytic pathway: membrane cargo and lipid requirements. *Mol. Biol. Cell*. 15:3542–3552. http://dx.doi.org/10.1091/mbc.E04-02-0151

Paterson, A.D., R.G. Parton, C. Ferguson, J.L. Stow, and A.S. Yap. 2003. Characterization of E-cadherin endocytosis in isolated MCF-7 and chinese hamster ovary cells: the initial fate of unbound E-cadherin. *J. Biol. Chem.* 278:21050–21057. http://dx.doi.org/10.1074/jbc.M300082200

Ponta, H., L. Sherman, and P.A. Herrlich. 2003. CD44: from adhesion molecules to signalling regulators. *Nat. Rev. Mol. Cell Biol.* 4:33–45. http://dx.doi.org/10.1038/nrm1004

Porat-Shliom, N., Y. Kloog, and J.G. Donaldson. 2008. A unique platform for H-Ras signaling involving clathrin-independent endocytosis. *Mol. Biol. Cell*. 19:765–775. http://dx.doi.org/10.1091/mbc.E07-08-0841

Powelka, A.M., J. Sun, J. Li, M. Gao, L.M. Shaw, A. Sonnenberg, and V.W. Hsu. 2004. Stimulation-dependent recycling of integrin beta1 regulated by ARF6 and Rab11. *Traffic*. 5:20–36. http://dx.doi.org/10.1111/j.1600-0854.2004.00150.x

Prosser, D.C., T.G. Drivas, L. Maldonado-Báez, and B. Wendland. 2011. Existence of a novel clathrin-independent endocytic pathway in yeast that depends on Rho1 and formin. *J. Cell Biol.* 195:657–671. http://dx.doi.org/10.1083/jcb.201104045

Puthenveedu, M.A., B. Lauffer, P. Temkin, R. Vistein, P. Carlton, K. Thorn, J. Taunton, O.D. Weiner, R.G. Parton, and M. von Zastrow. 2010. Sequence-dependent sorting of recycling proteins by actin-stabilized endosomal microdomains. *Cell*. 143:761–773. http://dx.doi.org/10.1016/j.cell.2010.10.003

Radhakrishna, H., and J.G. Donaldson. 1997. ADP-ribosylation factor 6 regulates a novel plasma membrane recycling pathway. *J. Cell Biol.* 139:49–61. http://dx.doi.org/10.1083/jcb.139.1.49

Radhakrishna, H., O. Al-Awar, Z. Khachikian, and J.G. Donaldson. 1999. ARF6 requirement for Rac ruffling suggests a role for membrane trafficking in cortical actin rearrangements. *J. Cell Sci.* 112:855–866.

Richardson, S.C., S.C. Winistorfer, V. Poupon, J.P. Luzio, and R.C. Piper. 2004. Mammalian late vacuole protein sorting orthologues participate in early endosomal fusion and interact with the cytoskeleton. *Mol. Biol. Cell*. 15:1197–1210. http://dx.doi.org/10.1091/mbc.E03-06-0358

Roberts, E.A., J. Chua, G.B. Kyei, and V. Deretic. 2006. Higher order Rab programming in phagolysosome biogenesis. *J. Cell Biol.* 174:923–929. http://dx.doi.org/10.1083/jcb.200603026

Sandvig, K., S. Pust, T. Skotland, and B. van Deurs. 2011. Clathrin-independent endocytosis: mechanisms and function. *Curr. Opin. Cell Biol.* 23:413–420. http://dx.doi.org/10.1016/j.ceb.2011.03.007

Song, J., Z. Khachikian, H. Radhakrishna, and J.G. Donaldson. 1998. Localization of endogenous ARF6 to sites of cortical actin rearrangement and involvement of ARF6 in cell spreading. *J. Cell Sci.* 111:2257–2267.

Sunio, A., A.B. Metcalf, and H. Krämer. 1999. Genetic dissection of endocytic trafficking in *Drosophila* using a horseradish peroxidase-bride of sevenless chimera: hook is required for normal maturation of multivesicular endosomes. *Mol. Biol. Cell*. 10:847–859.

Szebenyi, G., B. Hall, R. Yu, A.I. Hashim, and H. Krämer. 2007. Hook2 localizes to the centrosome, binds directly to centriolin/CEP110 and contributes to centrosomal function. *Traffic*. 8:32–46. http://dx.doi.org/10.1111/j.1600-0854.2006.00511.x

Traub, L.M. 2009. Tickets to ride: selecting cargo for clathrin-regulated internalization. *Nat. Rev. Mol. Cell Biol.* 10:583–596. http://dx.doi.org/10.1038/nrm2751

Walenta, J.H., A.J. Didier, X. Liu, and H. Krämer. 2001. The Golgi-associated hook3 protein is a member of a novel family of microtubule-binding proteins. *J. Cell Biol.* 152:923–934. http://dx.doi.org/10.1083/jcb.152.5.923

Walseng, E., O. Bakke, and P.A. Roche. 2008. Major histocompatibility complex class II-peptide complexes internalize using a clathrin- and dynamin-independent endocytosis pathway. *J. Biol. Chem.* 283:14717–14727. http://dx.doi.org/10.1074/jbc.M801070200

Weigert, R., A.C. Yeung, J. Li, and J.G. Donaldson. 2004. Rab22a regulates the recycling of membrane proteins internalized independently of clathrin. *Mol. Biol. Cell*. 15:3758–3770. http://dx.doi.org/10.1091/mbc.E04-04-0342

Xu, L., M.E. Sowa, J. Chen, X. Li, S.P. Gygi, and J.W. Harper. 2008. An FTS/Hook/p107(FHIP) complex interacts with and promotes endosomal clustering by the homotypic vacuolar protein sorting complex. *Mol. Biol. Cell*. 19:5059–5071. http://dx.doi.org/10.1091/mbc.E08-05-0473

Yan, Y., S. Vasudevan, H.T. Nguyen, and D. Merlin. 2008. Intestinal epithelial CD98: an oligomeric and multifunctional protein. *Biochim. Biophys. Acta*. 1780:1087–1092. http://dx.doi.org/10.1016/j.bbagen.2008.06.007

Zimmermann, P., Z. Zhang, G. Degeest, E. Mortier, I. Leenaerts, C. Coomans, J. Schulz, F. N'Kuli, P.J. Courtoy, and G. David. 2005. Syndecan recycling [corrected] is controlled by syntenin-PIP2 interaction and Arf6. *Dev. Cell*. 9:377–388. (published erratum appears in *Dev. Cell.* 2005. 9:721) http://dx.doi.org/10.1016/j.devcel.2005.07.011

Zöller, M. 2011. CD44: can a cancer-initiating cell profit from an abundantly expressed molecule? *Nat. Rev. Cancer*. 11:254–267. http://dx.doi.org/10.1038/nrc3023